

## **General Disclaimer**

### **One or more of the Following Statements may affect this Document**

- This document has been reproduced from the best copy furnished by the organizational source. It is being released in the interest of making available as much information as possible.
- This document may contain data, which exceeds the sheet parameters. It was furnished in this condition by the organizational source and is the best copy available.
- This document may contain tone-on-tone or color graphs, charts and/or pictures, which have been reproduced in black and white.
- This document is paginated as submitted by the original source.
- Portions of this document are not fully legible due to the historical nature of some of the material. However, it is the best reproduction available from the original submission.

FINAL REPORT

THEORETICAL STUDIES OF SOLAR OSCILLATIONS

NASA Grant NSG-7342

Grant period 10/1/76-9/30/80

(NASA-CR-163611) THEORETICAL STUDIES OF  
SOLAR OSCILLATIONS Final Report, 1 Oct.  
1976 - 30 Sep. 1980 (California Inst. of  
Tech.) 64 p HC A04/MF A01 CSCL 03B

N80-34326

Unclas  
G3/92 28936

Peter Goldreich

Principal Investigator

Professor of Planetary Science & Astronomy

California Institute of Technology

Pasadena, California 91125

J. David Bohlin

Technical Officer

National Aeronautics & Space Administration

Headquarters - ST/5

Washington, D.C. 20546



### RESEARCH SUMMARY

Goldreich and Keeley continued their investigation of possible sources for the excitation of the solar 5-minute oscillations. They also applied their linear non-adiabatic stability code to a preliminary study of the solar g-modes with periods near 160 minutes. In spite of a great deal of hard work, no definitive conclusions concerning the excitation of these modes were reached. Reports of the early stages of this work were presented at several conferences by Keeley and are included in the publications listed below.

The excitation of the 5-minute oscillations by turbulent stresses in the convection zone remains a viable possibility. However, the power spectrum of the oscillations calculated by assuming that the turbulence is that given by mixing length theory does not agree very well with observation. In particular, the theoretical power spectrum declines too slowly with decreasing frequency and too rapidly with decreasing horizontal wave number to provide a good match to the observations. In spite of these difficulties, these calculations do give oscillation amplitudes which are of the correct order of magnitude.

Theoretical calculations do not offer much support for the identification of the 160 minute global solar oscillation (reported by several independent observers) as a solar g-mode. The computations indicate that radiative dissipation in the

region below the convection zone exceeds the driving produced in the ionization zones by the  $\kappa$ -opacity mechanism. The large mass involved in these g-modes implies that even the substantial excitation they received from turbulent stresses produces a surface velocity amplitude which is much smaller than the observationally determined value. The most promising source of instability is nuclear driving, but this appears to be insufficient to overcome radiative damping.

Our most recent work has been an attempt to reconcile mixing-length theory with the results of the calculations of linearly unstable normal modes. Here we have made a significant advance. Our calculations show that in a convective envelope prepared according to mixing length theory, the only linearly unstable modes are those which correspond to the turbulent eddies which are the basic element of the heuristic mixing length theory. We intend to write a paper entitled "In Defense of the Mixing Length Hypothesis." In addition to announcing the result just mentioned, we shall describe how the surface velocity field is related to that at depth in the convection zone. Ultimately, we hope our study will provide an explanation for the solar supergranulation.

PUBLICATIONS

1. Goldreich, P. and Keeley, D.A., 1977, Solar Oscillations, Comments on Astrophysics, VII, 35.
2. Keeley, D.A., 1978, Some Problems in the Theory of Global Solar Oscillations, in Proceedings of the Symposium on Large Scale Motions on the Sun, Sacramento Peak Observatory.
3. Keeley, D.A., 1978, A Preliminary Attempt to Interpret the Power Spectrum of the Solar Five Minute Oscillations in Terms of the Global Oscillation Model, in Current Problems in Stellar Pulsation Instabilities, NASA Technical Memorandum 80625.
4. Keeley, D.A., 1979, Excitation of Solar G-Modes with Periods Near 160 Minutes, in Lecture Notes in Physics #125, Nonradial and Nonlinear Stellar Pulsation. Tucson, 1979. Ed. H.A. Hill and W.A. Dziembowski, Springer-Verlog.
5. Goldreich, P. and Keeley, D.A., 1980, In Defense of the Mixing Length Hypothesis, in preparation.

## Solar Oscillations

### Introduction

Current knowledge of the internal structure of the sun is almost entirely based upon theoretical calculations of solar models. Confidence in these models has been shaken by their failure to predict the solar neutrino flux. The determination of the frequencies of the sun's normal modes would provide us with sensitive probes of the solar interior. If an appreciable number of low frequency modes were detected, the run of the basic variables  $p$ ,  $\rho$  and  $T$  could be deduced with only a little help from theory. Even the internal rotation of the sun would be subject to observation study through the splitting of the modal frequencies it produces. For the aforementioned reasons, recent claims of the detection of several long period solar oscillations have aroused considerable interest. We shall review the main observational results and related theoretical investigations.

### Classification

The normal modes of oscillation of the sun may be classified according to their angular eigenvalues  $l$  and  $m$  and the number of their radial nodes,  $n$ .† For each  $l$ , there is a mode whose radial displacement and pressure perturbation have no radial nodes. This mode is designated the fundamental- or f-mode. Modes of higher frequency than the f-mode are called pressure- or p-modes. The frequencies of the p-modes increase with increasing  $n$ . For large  $n$ , the p-modes resemble standing acoustic waves. The restoring force is predominantly due to pressure, the velocity is approximately radial and is confined near the solar surface. For  $l \neq 0$ , there is another sequence of modes whose frequencies are lower than that of the f-mode. These are the gravity- or g-modes. The frequencies of the g-modes decrease with increasing  $n$ . For large  $n$ , the restoring forces are largely due to

---

† For each  $l$  there are  $2l + 1$  nearly degenerate modes whose frequencies are slightly split by the sun's rotation

gravity which acts to reduce deviations of the surfaces of constant density from those of constant potential. The velocity is nearly horizontal and its amplitude peaks deep in the sun's interior.

### *Observations of Excited Normal Modes*

**Old results** The power spectrum of the photospheric radial velocity field shows a broad peak ( $\Delta P/P \sim 0.3$ ) which is centered at a period of approximately 5 minutes.<sup>1</sup> The 5-minute oscillations are properly interpreted as the superposition of many, non-radial p-modes.<sup>2,3,4</sup> All told there are more than  $10^6$  modes with periods between 4 and 6 minutes.<sup>5</sup> For example, some combinations of  $l$  and  $n$ , denoted by  $(l, n)$ , which give p-modes with periods near 5-minutes are  $(0, 20)$ ,  $(10, 17)$ ,  $(10^2, 7)$  and  $(10^3, 0)$ .

The solar granulation is the surface manifestation of turbulent convection. Turbulent convection may be thought of as the superposition of many unstable, non-linearly coupled, g-modes. The non-linear couplings among these unstable g-modes are so strong that the description of turbulent convection in terms of linear modes is generally not pursued.

**New results** In recent years, several groups have reported the detection of additional modes of solar pulsation. It has been announced that the power spectrum of the temporal variation of the solar diameter exhibits several peaks at periods between 20 and 60 minutes.<sup>6</sup> Such periods fall in the range expected for p-modes with small  $l$  and  $n$ . Indeed, some theoreticians have succeeded in matching the observed periods with those calculated from solar models.<sup>7,8,9</sup> If interpreted in terms of physical motions of the sun's surface layers, the diameter variations would imply surface velocities up to  $30 \text{ m s}^{-1}$ . These inferred velocities are in conflict with upper limits of order  $1 \text{ m s}^{-1}$  established by direct observation of the photospheric velocity field.<sup>10</sup> It has been suggested that the apparent diameter oscillations are largely due to periodic variations in limb brightness rather than to surface displacements.<sup>6</sup> This suggestion is difficult to reconcile with the small observational limits placed on atmospheric temperature oscillations.<sup>11</sup> Furthermore, we expect the sun's surface layers to respond rather stiffly to driving at periods much longer than the acoustic cutoff period of  $\sim 180 \text{ s}$ . This expectation is confirmed by detailed numerical calculations of nonadiabatic p-mode eigenfunctions. These eigenfunctions show that variations in limb brightness make a negligible contribution to the apparent changes of solar diameter.<sup>12</sup>

Two groups claim to have detected an oscillation of the solar surface with a period of 2 hours 40 minutes and a velocity amplitude of  $2 \text{ m s}^{-1}$ .<sup>13,14</sup> The pulsation period is too long for any solar p-mode and can only be accounted for by a solar g-mode such as the g-mode with  $l = 2, n = 11$ .<sup>7</sup> At first glance, the detection of this oscillation would appear to be totally convincing. Its discovery

was announced simultaneously by two independent groups, and no reports of conflicting observations have appeared in the astronomical literature. Nevertheless, closer scrutiny raises some doubts. One of the groups based their claim of discovery on only 2 days of data. The period, 2 hours 40 minutes, is exactly  $1/4$  of a day. Finally, only a single mode was detected with a period longer than 1 hour. Why is this mode so special since there are many solar g-modes with periods longer than 1 hour?

This brief description of the observational status of the detection of solar normal modes summarizes the published observations. It is not surprising, especially in a new and controversial subject such as ours, that rumors of additional significant observations abound. However, in our opinion it is too early to draw any firm conclusions concerning the validity of the claimed detections of solar oscillations with periods longer than 10 minutes.

Since the observational situation is murky and seems unlikely to be clarified in the near future, we turn to theory, that most unreliable of astronomical tools, to guide us. The theoretical goal is to estimate the energy in each of the solar normal modes.

### *Linear Stability Calculations*

Work in this area has largely been confined to studies of the p-modes. The prime difficulty is the lack of any trustworthy theory of time-dependent convection. Nonadiabatic, linear stability calculations which neglect the coupling between convection and pulsation predict instability for p-modes with  $P \gtrsim 5$  minutes.<sup>5,12</sup> The driving of the instability is due to the  $\kappa$ -mechanism which operates in the H ionization-H<sup>-</sup> opacity region just below the photosphere. The high frequency p-modes,  $P \lesssim 5$  minutes, are stabilized by radiative damping in the solar atmosphere. The precise frequency that separates stable from unstable modes is very uncertain and depends sensitively on poorly determined details of the atmospheric structure.

Unfortunately, the interaction between convection and pulsation does not appear to be negligible. In fact, an investigation that includes the effects of time-dependent convection finds that all of the p-modes are stable.<sup>12</sup> This investigation uses a model of time-dependent convection based on mixing length theory. The modes are stabilized by the mechanical damping due to turbulent viscosity in the convection zone. However, the calculated margin of stability is small and the uncertainties in the theoretical model for turbulent viscosity are considerable. Thus, it seems wisest to conclude that theoretical calculations are incapable of determining the linear stability of the solar p-modes.

One interesting corollary of the stability calculations is the determination of the quality factor, or  $Q$ , of the normal modes. The frequency width  $\Delta\omega$  of each

mode is related to the modal frequency  $\omega$  and to  $Q$  by  $\Delta\omega/\omega = 1/2Q$ . The frequency widths of the low order p-modes are much smaller than their frequency splittings due to the solar rotation. For example, the radial f-mode has  $\omega = 1.9 \times 10^{-3} \text{ s}^{-1}$ ,  $Q = 2 \times 10^9$  and thus  $\Delta\omega \sim 4 \times 10^{-13} \text{ s}^{-1}$ , while the rotation frequency of the solar surface  $\Omega \approx 2.7 \times 10^{-6} \text{ s}^{-1}$ .

There is an indirect argument which suggests that the low order p- and g-modes are not linearly unstable. It rests on the fact that the 'observed' amplitudes of these modes are so small. The reported radial displacements  $\Delta r/R_\odot \approx 10^{-5}$ . It is hard to imagine any non-linearities that might lead to the saturation of linearly unstable modes at these small amplitudes.

If we accept the preceding argument and conclude that the low-order p- and g-modes are linearly stable, we are still left with the problem of identifying their principal sources of excitation. Here we are guided by general thermodynamic principles. These tell us that sources of excitation are intimately linked to sources of damping. Since turbulent viscosity in the convection zone appears to be the principal damping mechanism for p-modes with  $P \gtrsim 5$  minutes, we are led to ask how convective turbulence might act as a source of excitation for these modes.<sup>15</sup>

#### *Stochastic Excitation of the p-Modes by Turbulent Convection*

There are two ways of viewing the interaction between turbulent convection and a p-mode. The turbulent convection may be described as the superposition of many unstable g-modes. The problem then reduces to one of calculating the non-linear couplings between one p-mode and two or more g-modes. The non-linear interactions among the g-modes broaden their frequencies so that resonance relations required for energy sharing between the p-mode and two or more g-modes are satisfied in many cases. Experience with non-linear mode coupling in other circumstances leads us to expect the energy of each p-mode to be comparable to the energy in those g-modes which couple most strongly to that particular p-mode. This last qualification is necessary because the unstable g-modes in turbulent convection do not attain energy equipartition. Most likely, the g-mode energy spectrum has the Kolmogoroff form.<sup>12,16</sup>

The other way of estimating the excitation of the p-modes by turbulent convection is more physical. Turbulent flows are always accompanied by a fluctuating stress field which acts as a source of acoustic radiation. In an unbounded medium, the dominant source term arises from the Reynolds stress and produces quadrupole radiation.<sup>17</sup> The bandwidth of the emitted acoustic radiation spans the frequencies of the eddies in the turbulent flow. In the sun, acoustic disturbances (the p-modes) are restricted to a discrete set of frequencies. Turbulent convection in the sun can only generate radiation at the frequencies

of these discrete modes. The rate at which turbulent convection pumps energy into each p-mode depends upon the modal frequency and the spectrum of the turbulence. A plausible estimate of the turbulent spectrum may be obtained from a combination of mixing length theory and the Kolmogoroff scaling.<sup>12,16</sup> Once the spectrum is chosen, it is a simple matter to calculate the rate of generation of modal energy. The steady state value of the energy in each p-mode is determined by a balance between the power radiated at the modal frequency and the mechanical dissipation of modal energy by turbulent viscosity. These interactions are such that the modal energy tends toward equipartition with the kinetic energy in a single turbulent eddy whose turnover time is comparable to the modal period. This simple picture is slightly complicated because the properties of the turbulence vary with depth in the convection zone. It is easy to show that the strongest interactions between a p-mode and the turbulent convection take place at the level where the turnover time of the largest eddies (assumed to have linear dimensions of order the pressure scale height) is equal to the modal period. Detailed calculations based on a standard solar model yield values for the energies in the radial modes that range from  $2 \times 10^{26}$  erg for the f-mode to  $2 \times 10^{24}$  erg for the p<sub>20</sub>-mode. The absolute values of the predicted modal energies depend sensitively on the convective velocity. To a fair approximation, the modal energies vary as the seventh power of the convective velocity (at fixed mixing length). Thus, until an accurate theory of turbulent convection is developed, it will not be possible to estimate the modal energies to better than a few orders of magnitude.

Once the energies in the p-modes are calculated, their surface velocity amplitudes may be predicted. The predicted velocities are disappointingly small. Typical values for the radial f-through p<sub>20</sub>-modes vary smoothly from  $10^{-2} \text{ cm s}^{-1}$  to  $6 \times 10^{-1} \text{ cm s}^{-1}$ . The increase of the predicted surface velocity with  $n$  reflects the fact that as  $n$  increases the p-modes become more strongly confined to the surface layers of the sun.

There is no escaping the fact that the predicted surface velocities of the p-modes are much smaller than the values inferred from the observations of the solar diameter. We see no hope of reconciling the theoretical and observational results. One or the other must be in error.

#### *The Five-minute Oscillations*

It has recently been established that the spectral power density of the 5-minute oscillations is concentrated in bands in the  $k_h, \omega$  plane.<sup>18,19</sup> Here  $k_h$  is the horizontal wave number and  $\omega$  is the angular frequency. The locations of these bands conform with theoretical predictions based on the assumption that the 5-minute oscillations are the superposition of many excited, non-radial p-modes.



The precise locations of the bands are sensitive to the specific entropy in the convection zone.<sup>20</sup> The observations are fit best by solar models which have convection zones of low specific entropy. Models of this type result if a high efficiency for sub-surface convection is assumed. These models have deep convection zones.

The mechanism that determines the excitation of the 5-minute oscillations is not firmly established. Several authors have proposed that the p-modes involved in the oscillations are linearly overstable.<sup>2,4,5</sup> The driving of this overstability is attributed to the  $\kappa$ -mechanism. Alternately, it is possible that the oscillations are stochastically excited by turbulent stresses in the convection zone. A crucial problem is the determination of the rate at which energy is shared among the p-modes involved in the 5-minute oscillations. The transfer of energy among the p-modes arises from their non-linear couplings. The most important couplings are within triplets of p-modes. Once the rate of energy sharing among the p-modes is estimated (a problem we are working on), it can be compared to the rate at which the p-modes share energy with the g-modes.

If the p-modes couple more strongly to the g-modes than they do to each other, then the amplitude and spectrum of the 5-minute oscillations would be due to the stochastic excitation of the p-modes by turbulent stresses in the convection zone. The high frequency cutoff of the spectrum could plausibly be attributed to the strong, radiative damping suffered by p-modes with  $P \lesssim 5$  minutes. Furthermore, we could reasonably conclude that the p-modes involved in the 5-minute oscillations were linearly stable. In the absence of mutual energy sharing, we would not expect unstable p-modes to saturate at the small amplitudes inferred from observation, nor would we expect the amplitudes to vary smoothly with  $l$  and  $n$  as observations suggest they do.<sup>19</sup>

On the other hand, if the coupling among the p-modes is stronger than the coupling of the p-modes to the g-modes, the possibility that at least some of the p-modes are linearly unstable would have to be seriously entertained. If the p-modes are unstable and strongly coupled, they would form a system that is similar to that of the g-modes involved in the turbulent convection.

PETER GOLDBREICH

*California Institute of Technology*

DOUGLAS A. KEELEY

*University of California at Santa Cruz*

#### References

1. R. B. Leighton, R. N. Noyes and G. W. Simon. *Astrophys. J.* **135**, 479 (1962).
2. R. K. Ulrich, *Astrophys. J.* **162**, 993 (1970).
3. J. Leibacher and R. I. Stein. *Astrophys. Lett.* **7**, 191 (1971).
4. C. L. Wolff, *Astrophys. J. Lett.* **177**, L87 (1972).
5. H. Ando and Y. Osaki. *Publ. Astron. Soc. Japan* **27**, 581 (1975).
6. H. A. Hill, R. T. Stebbins and T. M. Brown, *Proc. V. Intern. Conf. Atomic Masses and Fundamental Constants (Paris)*, 1975.
7. J. Christensen-Dalsgaard and D. O. Gough. *Nature*, **259**, 90 (1976).
8. I. Iken, Jr., and J. Mahaffy. *Astrophys. J.* **209**, L39 (1976).
9. C. A. Rouse. *Astron. Astrophys.* **55**, 477 (1977).
10. G. Grec and E. Fossat. *Astron. Astrophys.* **55**, 411 (1977).
11. W. Livingston, R. Milkey and C. Slaughter. *Astrophys. J.* **211**, 681 (1977).
12. P. Goldreich and D. A. Keeley. *Astrophys. J.* **211**, 934 (1977).
13. A. B. Severny, V. A. Kotov and T. T. Tsap. *Nature* **254**, 87 (1976).
14. J. R. Brookes, G. R. Isaak and H. B. van der Raay. *Nature* **259**, 92 (1976).
15. P. Goldreich and D. A. Keeley. *Astrophys. J.* **212**, 243 (1977).
16. E. A. Spiegel. *J. Geophys. Res.* **67**, 3063 (1962).
17. M. J. Lighthill. *Proc. Roy. Soc. Lond.* **A211**, 564 (1952).
18. F. L. Deubner. 1975, *Astron. Astrophys.* **44**, 371 (1975).
19. E. J. Rhodes, Jr., R. K. Ulrich and G. W. Simon. To be published (1977).
20. R. K. Ulrich and E. J. Rhodes, Jr. To be published (1977).

#### Acknowledgement

The work reported here has been supported by the NSF and by NASA.

**SOME PROBLEMS IN THE THEORY OF  
GLOBAL SOLAR OSCILLATIONS.**

**D. A. Keeley**

**A paper presented at the  
Symposium on Large Scale Motions  
on the Sun, Sacramento Peak  
Observatory, Sept. 1-2, 1977.**

**This work was supported in part by NASA.**

## I. Introduction

This paper presents a discussion of two of the important problems concerning solar oscillation modes. In § II the possible effect of the mechanical boundary condition on the low frequency P modes is reviewed, and some limits to these effects are discussed in the framework of a simple analytical model. In § III, a model for the excitation and damping of the 5 minute oscillations is discussed and some results of calculations are presented. § IV is a brief discussion of the global nature of the oscillations.

## II. The Boundary Condition Problem for Long-Period P-modes.

Hill's observations (1976) of long-period oscillations in the sun can be reconciled with low limits on the velocity amplitude if the amplitude of the temperature perturbation  $\delta T/T$  is much larger than the displacement amplitude  $\delta r/r$  at the atmospheric level of his observations. Observations of  $\delta T/T$  at lower levels of the atmosphere, in combination with Hill's inferred  $\delta T/T$ , lead to constraints on the gradient of  $\delta T/T$ . The requirements are inconsistent with the results of conventional model calculation for the radial modes and low P modes, which have generally been assumed to be the most likely candidates. However, the model calculations are extremely sensitive to the boundary conditions, and it has been suggested that therein lies the resolution of the problem. Another possibility, which Hill has raised at this symposium, is that the oscillations may be g modes with spherical harmonic number  $L$  in the range 20-50. Preliminary calculations of these modes also appear to be inconsistent with the observations.

### a) Radial Modes

Typical results of a conventional calculation for the fundamental radial mode are shown in figure 1. The fractional temperature perturbation is shown as a function of optical depth  $\tau$ , and the phase angle relative to the displacement amplitude is indicated at various points

along the curve. The last point in the model cannot be shown on the optical depth scale, but the amplitude and phase are indicated in the upper left of the diagram. The last plotted point is at an optical depth corresponding roughly to the temperature minimum. The normalization of  $\frac{\delta T}{T}$  is such that  $\delta r/r = 1$  at the outer boundary of the model. Over the range shown,  $\delta r/r$  varies by less than 1%. For  $\tau > 1$ , the phase angle gradually approaches  $180^\circ$ , and the amplitude approaches the adiabatic value by the point where the temperature of the model is about  $20,000^\circ$ .

The temperature perturbation was calculated from  $\frac{dE}{dt} + \frac{P}{\rho} \nabla \cdot \vec{\pi} = -\frac{1}{\rho} \nabla \cdot \vec{F}$ , in which the flux and displacement perturbations, and thus the real and imaginary parts of the eigenvalue, were calculated simultaneously.

The mechanical boundary condition applied to the model was that the pressure perturbation vanish in the region outside the last boundary in the system of difference equations. It then follows that  $\nabla \cdot \delta \vec{r}$  in the last zone of the model is given by

$$\nabla \cdot \delta \vec{r} = \frac{\Delta m}{4\pi r^2 \rho_{\Pi}} (\omega^2 + \frac{4g}{r}) \delta r ,$$

in which  $p$  is the pressure,  $g$  is the gravitational acceleration, and  $\Delta m$  is the mass associated with the last boundary. The hydrostatic model was calculated with  $P = 0$  in the exterior zone, and thus

$$\nabla \cdot \delta \vec{r} = \frac{H}{c^2} (\omega^2 + \frac{4g}{r}) \delta r ,$$

where  $c$  is the soundspeed and  $H$  is the pressure scale height.

A simple analytic model suffices to demonstrate the importance of the boundary condition. For simplicity consider a plane parallel atmosphere with a constant pressure scale height. Then the displacement amplitude takes the form

$$\delta r = A \exp(k^+ z) + B \exp(k^- z) ,$$

in which  $A$  and  $B$  are constants, and  $z$  is the height measured above some

arbitrary reference level. The wave numbers  $k^{\pm}$  are given by

$$k^{\pm} = Y^{-1} \left( 1 \pm (1 - 2\mu_0^2 Y)^{\frac{1}{2}} \right),$$

in which  $Y \equiv 2H$ , and  $\mu_0^2 \equiv \omega^2 / (\Gamma_0 g)$ . The waves are evanescent if  $k$  is real. The solutions  $k^{\pm}$  correspond to incoming and outgoing waves, respectively. For  $\omega \approx 2 \times 10^{-3}$ , roughly the frequency of the fundamental radial mode,  $\mu_0^2 Y \ll 1$  if the scale height is much less than  $10^{10}$  cm. Thus, in the vicinity of the temperature minimum, where most model calculations are terminated,

$$k^+ \approx H^{-1}, \quad k^- \approx \omega^2 H / c^2.$$

The wave-number  $k^+$  of the incoming evanescent wave is several orders of magnitude larger than  $k^-$ . The boundary condition used in the model calculation essentially amounts to allowing only the outgoing wave. (The  $4g/r$  term has been omitted because of the plane parallel assumption.)

The point made by Hill et al. (1976) is that the adiabatic part of the temperature perturbation is given by

$$\frac{\delta T}{T} = -(\Gamma_0 - 1) \frac{\delta r}{\delta z} = -(\Gamma_0 - 1)(A k^+ + B k^-)$$

if the point of interest is taken to be  $z = 0$ . Thus if the coefficients of the two waves are roughly equal in the displacement function, then the temperature perturbation is completely dominated by the incoming evanescent wave, and is very much greater than the displacement amplitude  $\delta r/r$ . Thus observations made in the vicinity of the temperature minimum might well show a large temperature amplitude. Lower in the atmosphere, the amplitude of the incoming wave has decayed by a factor of the pressure ratio between the two points, since  $k^+ \sim H^{-1}$ , and the corresponding temperature perturbation will be much smaller.

The question to be decided is whether in fact a significant amount of the incoming wave can be present. Such a wave can exist in principle

if there are any reflecting layers above the point in question. It can be demonstrated within the context of the simple analytical model above that for a single reflecting boundary with only an outgoing wave beyond it,  $|A/B| < 1$  at the boundary. This result is obvious from energy considerations if the region interior to the boundary allows the waves to propagate; it can also be shown simply for the evanescent case.

In figure 2 the relationship between  $k$  and  $Y$  is plotted. Consider now a situation in which a boundary separates regions of different  $Y$ . Then if  $k^*$  is the wave number of the outgoing wave in the exterior region,

$$\frac{A}{B} = - \frac{(k^- - k^*)}{(k^+ - k^*)}$$

Both  $k^-$  and  $k^*$  must lie on the lower curve, and  $k^+$  is on the upper curve at the same  $Y$  value as  $k^-$ . The curve  $1/Y$  is halfway between the upper and lower branches. It is immediately obvious from the diagram that  $k^- - k^*$  is bounded, whereas  $k^+ - k^*$  is not, so that if the  $Y$  corresponding to  $k^-$  is not too close to the critical point,  $|A/B| < 1$  is easily satisfied. A little algebra shows that in fact it is satisfied for any choice of  $k^*$  whatsoever, in the evanescent or propagating region, and for any pair  $k^\pm$  in the evanescent region.

In the case at hand,  $k^+ \gg k^-, k^*$ , and  $|A/B| \sim k^-/k^+$ . In other words,  $k^+A \approx k^-B$ , which means that the two waves contribute roughly equally to the temperature amplitude at the boundary. Therefore a single reflecting boundary near the temperature minimum will never result in  $\delta T/T \gg \delta r/r$ .

Unfortunately, it is clear that a situation involving more than one boundary cannot yield so clear-cut a result. Just as a coating on a lens can change the ratio of reflected to transmitted energy drastically, a similar situation occurs for evanescent waves. Indeed, for suitable choice of scale heights in the exterior, middle, and interior regions one can arrange to have a purely incoming evanescent wave in the interior, a purely outgoing one in the exterior, and a mixture in the middle. Thus if one will admit the possibility of more than one reflecting boundary, the question is still open.

A calculation which goes fairly far towards closing it again is described below. An adiabatic eigenfunction calculation was performed on a solar model with a chromosphere extending out to  $T \sim 2 \times 10^4$ ,  $P \sim 10^{-3}$ , supplied by Roger Ulrich. The boundary condition applied was the same as before. The result was a displacement eigenfunction in which  $\delta r/r$  changed about 3% from the temperature minimum to the outer point, and its derivative was essentially the same as that found in the previous model calculation. This demonstrates the important point that nothing drastic happens to the eigenfunction in the vicinity of the temperature minimum. That region does not act like a pair of reflecting boundaries, or at least, not a pair with serious consequences for the eigenfunction. The second point is that the region of the temperature minimum is seen to be separated from any other potentially-troublesome regions by at least six orders of magnitude in the pressure, over which any incoming evanescent wave would have decayed by roughly this same factor.

Thus it seems rather unlikely that the incoming evanescent wave can dominate the temperature perturbation amplitude at or below the temperature minimum.

The arguments above apply strictly to the adiabatic part of the temperature perturbation. In principle it is possible to do a full non-adiabatic calculation of a model including a chromosphere, but in practice this can not be done without a good description of the heating and cooling processes, and their response to perturbations. An estimate of the possible effect of the radiative processes can be obtained in the following way. In a plane-parallel atmosphere the condition of no incoming radiation gives a relation between the energy density and the flux as  $\tau \rightarrow 0$ . If this relationship is perturbed about an equilibrium situation in which  $\nabla \cdot \mathbf{F}$  (radiative) = 0, and applied at small optical depth to a model calculation, the dominant terms may be obtained from the condition  $\delta B = \frac{1}{4\pi\kappa} \delta \left( \frac{\nabla \cdot \mathbf{F}}{\rho} \right)$ , in which  $B$  is the Planck function and  $\kappa$  is the opacity. This equation, along with the expression for  $\delta T/T$  given by the heat equation, leads to  $\frac{\delta T}{T} = \frac{-(r_3 - 1) \nabla \cdot \delta \mathbf{F}}{(1 + \frac{16\pi B \kappa}{\omega C_v T})}$ , where  $i = (-1)^{1/2}$  and  $C_v$  is the specific heat in ergs/gm °K. Thus the total temperature perturbation is written as its adiabatic value divided by a factor which has magnitude  $> 1$  in all cases. In the case of the solar model for which  $\delta T/T$  was shown in figure 1, the factor in the denominator takes the value  $1 - 4.34i$ , and the amplitude and phase it predicts for  $\delta T/T$  are 1.85 and  $-103^\circ$ , as compared to 1.70 and  $-98^\circ$  obtained by the model calculation in which some smaller terms were also included.

In the presence of a non-radiative heating mechanism, the expression for  $\delta T/T$  from the heat equation involves perturbations of the non-radiative contribution to the flux, and cannot be estimated without a more detailed discussion of such mechanisms.

Besides the neglect of non-radiative heating and cooling mechanisms in the magnitude of  $\delta T/T$ , another criticism could be directed at the treatment of radiative transport in optically-thin regions. Whether these holes in



current discussion are large enough to accommodate the temperature perturbation eigenfunction suggested by Hill's observations is unknown. It seems fairly likely that purely adiabatic contributions to  $\delta T/T$  are insufficient.

#### b) Non-radial Modes

The situation for non-radial modes is considerably more complex. The  $k(Y)$  relation for this case is  $k^2 = Y(1 \pm (1 - 2\mu^2 Y + k_h^2 Y^2)^{1/2})$ , in which  $k_h = [L(L+1)/R^2]^{1/2}$  is the horizontal wave number, and  $\mu^2 = \mu_0^2 + k_h^2/\mu_0^2$ .  $\Gamma_1^{-1}(1 - \Gamma_1)$

If  $1 - \Gamma_1^{-1} < \mu_0^2/k_h < \Gamma_1^{-1}$  there is no propagation region for any value of  $Y$ . The  $k(Y)$  relation is shown in figure 3. The reflection coefficient is much more complicated than in the radial case, and it is more convenient to deal directly with the coefficients of the Lagrangian pressure perturbation.

If 
$$\frac{\delta P}{P} = A' \exp(k^+ z) + B' \exp(k^- z)$$

in the interior region, and  $\delta P/P = C' \exp(k^{*-} z)$  in the exterior, then continuity of  $\delta P/P$  and the radial displacement at the boundary yield the result

$$\frac{A'}{B'} = - \frac{\left[ \left( \frac{1 - \frac{\omega_L^2}{\omega^2}}{k^- - \frac{k_h^2 g}{\omega^2}} \right) - \left( \frac{1 - \frac{\omega_L^{*2}}{\omega^2}}{k^* - \frac{k_h^2 g}{\omega^2}} \right) \right]}{\left[ \left( \frac{1 - \frac{\omega_L^2}{\omega^2}}{k^+ - \frac{k_h^2 g}{\omega^2}} \right) - \left( \frac{1 - \frac{\omega_L^{*2}}{\omega^2}}{k^* - \frac{k_h^2 g}{\omega^2}} \right) \right]}$$

Here  $\omega_L^2 = c^2 k_h^2$ , and \* refers to quantities outside the boundary.

A simple case for which  $|A'/B'| \gg 1$  is obtained by choosing  $\omega_L^* = \omega$ . The reflection coefficient reduces to  $\frac{A'}{B'} = -\left(\frac{k^+ - k^{+*}}{k^- - k^{*-}}\right)$ . It is clear from figure 3 that this ratio can be large.

For the case of p modes with  $L \leq 20$ , model calculations including the chromosphere showed no sign of significant reflection in the region between the temperature minimum and the top point in the model. Higher  $L$  p-modes do not have frequencies in the range of interest. As in the radial mode case, the buffer provided by a factor of  $10^6$  in pressure between the last point in the model and the region of observation suggests that it is unlikely that there can be a strong reflected wave in the region of the temperature minimum. Of course, this conclusion has the same weaknesses as in the radial case.

Gravity wave modes with  $L \sim 20$ ,  $\omega \sim 2 \times 10^{-3}$  have large amplitude even within 10% of the center of the sun, and complete solar models are required for a discussion of their nature. The chromosphere model supplied by Ulrich, patched onto an interior model with a reasonably compatible equation of state, was used for an investigation of the g modes.

The mode at ( $L = 20$ ,  $\omega \approx 2 \times 10^{-3}$ ) had 16 nodes in  $\delta r/r$ . (Modes with higher  $L$  at the same  $\omega$  have more nodes and thus are increasingly difficult to calculate accurately by numerical techniques.) Both horizontal and vertical displacements varied quite slowly with radius above the surface of the convection zone and through the temperature minimum. Only in the immediate vicinity of the outer boundary point was there any significant contribution from the reflected wave. At ( $L = 30$ ,  $\omega = 2.5 \times 10^{-3}$ ) and ( $L = 50$ ,  $\omega = 3 \times 10^{-3}$ ) the behaviour of the eigenfunctions in the surface region was quite similar. The main difference came in the interior, where the amplitude was much higher relative to that at the surface; the result is that a kinetic energy orders of magnitude larger than is present in all the 5 minute modes combined, would be necessary to produce a velocity of 1 cm/sec at the surface.

These results suggest that the g modes are not significantly more favorable than the p modes as an explanation of the observations.

### III. Excitation and Damping of the Five Minute Oscillations.

The possibility that the observed oscillations in the period range 3 - 10 minutes could be excited by turbulence in the convection zone has been discussed by Goldreich and Keeley 1977. At the time of writing,

eigenfunctions for the non-radial modes which dominate at these periods, were not available to the authors, so only a crude estimate could be made of the excitation to be expected. Extensive calculations of adiabatic eigenfunctions, and the degree of excitation to be expected under various assumptions about the solar convection zone have now been done; some of the initial results are presented below.

One simple way of looking at the basic process is that the turbulent eddies generate acoustic energy over a broad range of frequencies determined by the size and turn-over time of the eddies, and their lifetimes as identifiable swirls. This acoustical energy constitutes an excitation of the normal modes of the sun as a whole. Alternately, the turbulent convection may be regarded as an excitation of a large number of unstable gravity-wave modes, very strongly non-linearly coupled to each other, and more weakly coupled to the P modes which dominate the 5 minute oscillations, and which are assumed to be accurately represented as linear oscillations. The latter approach, which treats the g and p modes on an equal footing, is more precise, but far less tractable than the former. Thus the first picture was used as the basis for the calculations.

Basically, what is done is to imagine that the properties of the turbulence are given, and not much influenced by the oscillations. The effect of the turbulence on the p modes is represented by inhomogeneous terms in the otherwise usual differential equations for the normal modes. The space and time behavior of the inhomogeneous terms is describable only in terms of the statistical properties of the turbulence. Conceptually, the problem is rather similar to that of Brownian motion of a particle in a harmonic oscillator potential. In the Brownian motion problem, the oscillator comes to energy equipartition with the molecules. The solar situation is more complicated

because it begins with a partial differential equation. However, in the limit where the turn-over time of the eddies is less than some numerical factor times the period of the oscillator (essentially the same as the assumption that the velocity of the Brownian particle changes negligibly on the timescale of the individual hits by molecules) the results obtained can be interpreted in terms of the normal mode coming to approximate energy equipartition with eddies having turnover-times approximately resonant with the normal mode. This bias towards one particular component of the turbulence presumably arises because of the assumption of a Kolmogoroff spectrum to describe the velocity at a given length scale; the kinetic energy resides mostly in the larger eddies. In the solar case, the dominant eddies in much of the convection zone (assumed to have size  $\sim$  scale height) have timescales much longer than 10 minutes. It is assumed that these eddies are ineffective in exciting short-period modes. However, even at such places in the convection zone, there are smaller-scale eddies, with shorter timescales, which can provide effective excitation. Of course, because of their smaller size, they have less kinetic energy to share with the normal mode.

The final amplitude of the oscillator depends on the balance between the energy added by the fluctuating forces, and the damping mechanisms. These are directly related, since the fluctuating forces which increase the kinetic energy of a normal mode from zero to the equilibrium value are also the origin of the frictional forces which reduce to the equilibrium value, the energy of a mode that initially is excited above that value. For this reason, the discussion necessarily turns to the dissipation of normal mode energy by turbulence. The excitation and dissipation can be treated together in the Brownian motion problem, but this has not been done for the

problem at hand. Instead, the effect of the turbulence has been modelled in terms of a turbulent viscosity coefficient. In keeping with the assumption made earlier with regard to excitation, it has been assumed that turbulent eddies with turn-over times greater than the oscillation period are ineffective in providing a damping force. The main damping then comes from the largest turbulent eddies which satisfy the time-scale requirement; these are precisely the ones which are most effective in exciting the modes. A further complication in the solar problem, which could have important consequences, is the presence of other damping and excitation mechanisms which also provide linear damping in the equation of motion for the normal modes.

The present calculations have been carried out using adiabatic eigenfunctions, and the excitation energy has been calculated assuming turbulent damping only. The radiative contribution to the damping (or excitation) is currently being investigated. Implications of the radiative damping constants for the present calculations are discussed later.

The eigenfunction and excitation energy are used to determine the surface velocity for each mode in the frequency range of interest. The number of normal modes involved is quite large. For example, between wave numbers of  $.285 \text{ (Mm)}^{-1}$  and  $.43 \text{ (Mm)}^{-1}$  there are about 400,000 modes with periods in the range of 3 minutes to 10 minutes. It has been assumed that the velocities add incoherently, so the sum of the squares has been taken to determine the total velocity.

#### a) Results of the Calculations

The rms velocity estimated earlier on the basis of knowledge of radial eigenfunctions only, was about a factor of 40 below the observed value of about 0.4 km/sec. With the non-radial mode calculation, the ordinary

mixing-length theory with  $\ell/H = 1$  gives 0.11 km/sec. For  $\ell/H = 2$ , the result is 0.23 km/sec. Thus it still falls short by a factor of about 4 in the energy required.

The results are rather sensitive to the velocity predicted by the mixing-length theory. Let  $\lambda$  be the scale and  $v_\lambda$  be the velocity of the eddies which make the dominant contribution to a given mode. Then the total energy of such an eddy is  $E \sim \lambda^3 v_\lambda^2$ . The timescale  $\tau_\lambda = \lambda/v_\lambda$  is to be held constant as the mixing length velocity is varied, since the main contribution comes from resonant eddies. Assuming a Kolmogoroff spectrum,  $v_\lambda/v_\ell = (\lambda/\ell)^{1/3}$  where  $\ell$  is the mixing length and  $v_\ell$  is the convective velocity given by mixing-length theory. From these relationships it follows that  $E \sim v_\ell^{7.5}$  if  $\tau_\lambda$  is held fixed. Thus a relatively small error in the convective velocity predicted by the mixing-length theory can make a large difference to the excitation energy, since the excitation energy is roughly proportional to the energy of the resonant eddies.

Figure 4 shows the excitation energy of the lowest-frequency mode at a given horizontal wave number. The spherical harmonic index  $L \equiv kR$ , where  $k$  is the horizontal wave number and  $R$  is the solar radius. The results are also shown if the mixing-length velocity is arbitrarily multiplied by a scale factor of 2. For the mixing-length unity model, the extra factor of two leads to an rms surface velocity of .47 km/sec., and for the mixing-length two model, 1.36 km/sec. The range of periods corresponding to the wave numbers shown is 10 minutes down to about 4 minutes. The excitation energy as a function of frequency, for  $L = 300$  ( $k \approx .43(\text{Mm})^{-1}$ ) is shown in figure 5. Each symbol represents a single normal mode, with the number of radial modes increasing with frequency. The large effect of an increase in the mixing

length is due in part to a higher density in the outer part of the convection zone, where the main contribution to these short period modes arises.

The actual surface  $v^2$  is shown in figures 6 and 7. Note especially that although the excitation energy at a given wave-number is a decreasing function of frequency, the surface velocity increases at first, because the kinetic energy of the higher modes is more favorably distributed. Finally, in figures 8 and 9, the observable energy is shown over a range of wave numbers and frequencies. Again, although the excitation energy of the high L modes is lower, much less kinetic energy is required for them to show a given surface velocity. In all cases the surface point is at a low optical depth  $\sim 10^{-3}$  to  $10^{-4}$ . If they were plotted at  $\tau = 1$ , then the high L modes, and the low L but high frequency modes would have somewhat lower velocities. Note that at  $L = 1500$ , only 2 different modes fall in the appropriate frequency range, whereas at  $L = 200$  there are 11. This is more than compensated by the  $(2L + 1)$ -fold degeneracy of the modes, so that more than half the total power is contributed by wave numbers above  $L = 1000$ .

In general, the results are fairly encouraging for the model. Ulrich and Rhodes (1977) have suggested, on the basis of observations of the normal mode frequencies as a function of wave numbers, the mixing length parameter may be as high as 2. This would put the velocity predicted by the theory within a factor of two of the observations, without any tampering with the convective velocity. Since the theory predicts the energy as a function of frequency and horizontal wave number, it can be compared in great detail with observations such as Ulrich's. Unfortunately, his complete set of data is not yet reduced, and the noise level in the part that is, is rather high. There is a possibility that the theory does not give a sharp enough increase in energy with increasing frequency, near 10 minutes period.

There are several important loose ends, and limitations, in the present calculations. Most of the excitation comes from the upper part of the convection zone where the timescales for the large eddies are not too long. This region in particular is likely to be sensitive to the convection theory. The velocities in the models used for the calculations presented here are surprisingly close to those in one of Ulrich's models, except for the outer scale height or so, in which they differed by as much as 50%. In all cases checked, less than about 25% of the excitation was produced in the discrepant region.

The theory could easily be incorrect in the assumptions which were made concerning the spatial and temporal correlation functions, and the spectrum of the turbulence. If the turbulent dissipation had been calculated directly by the same type of argument as the excitation rate, then there may have been more opportunity for errors to cancel. The turbulent viscosity coefficient was written simply as  $v_\lambda \lambda$ , where  $\lambda$  is the scale of the largest eddy which has a turnover time  $\tau_\lambda < \omega^{-1}$ . Any extra numerical factor multiplying the viscosity, changes the excitation energy by the same factor, according to the present method of calculation.

The calculations are incomplete because other damping mechanisms have not been included. The modes with periods shorter than about three minutes have been completely omitted because such modes are propagating rather than evanescent, in the vicinity of the temperature minimum. Thus they are expected to be damped quite strongly. The exact effect on the high-frequency end of the spectrum has not been calculated; this may be especially important at high wave-number, since much of the power is in those modes. Ando and Osaki (1975) calculated radiative damping rates, assuming that convection plays no role whatsoever. Unfortunately, the convective timescales



in the sun cover the range of periods of interest. Radial mode calculations with a simple treatment of time-dependent convection show that the convection may make the difference between a linearly unstable mode, and a stable one. Calculations are currently underway to explore the situation for non-radial modes. Ando and Osaki find linear instability over a wide range of modes involved in the 5 minute oscillations. This in itself is a little disturbing, unless some mechanism for limiting their amplitude to  $\delta r/r \sim 10^{-6}$  can be found.\* Unfortunately, the damping of the modes in this frequency range is very sensitive to the flux boundary condition (and possibly the treatment of radiative transport in the atmosphere). In the same approximation as discussed earlier, the perturbation of the flux divergence is given at the boundary point by 
$$\delta\left(\frac{\nabla \cdot \vec{F}}{\rho}\right) \left[ \frac{1}{4\pi K} + \frac{4B}{1\omega C_V T} \right] = -4B(\Gamma_3 - 1) \nabla \cdot \delta \vec{F},$$
 where  $i = (-1)^{1/2}$ . For the frequency range of interest, the two terms on the left are comparable, and so the phase of  $\delta(\nabla \cdot \vec{F}/\rho)$  is sensitive to  $\omega$ , and to the properties of the atmosphere. Although the radiative dissipation for  $\tau < 1$  is not very large, the actual flux perturbation at  $\tau \gg 1$  is strongly influenced by the magnitude and phase determined by the boundary condition. Since almost all the radiative excitation takes place in the layers at the top of the convection zone, the boundary condition has a very strong effect on the linear stability of the normal modes.

It was noted that in the radial calculations of the mixing-length unity model, the turbulent damping rates were comparable to radiative excitation rates from a period of an hour down to 5 minutes. For the non-radial modes, this situation also holds, if the calculations of Ando and Osaki are reasonable estimates. In fact, there are modes which are slightly unstable in the linear sense, in spite of the turbulent viscosity. If the turbulent damping is almost cancelled out by radiative excitation, then the steady-state

---

\* Hill has pointed out in this symposium that the opacity perturbation  $\delta K/K$  is large enough for non-linear effects to be important when the temperature perturbation is summed over all the modes involved in the five minute oscillations. This may be capable of increasing the rate at which energy is dispersed among the modes as a result of the non-linear coupling.

turbulent excitation energy of the mode will be much larger than the estimates given above. The turbulent damping rates of the mixing-length two model are not grossly different from those for mixing-length unity. However, those in which the convective velocity is artificially scaled up by a factor of 2 are roughly an order of magnitude higher.

Direct observations of the damping times of the modes would be very interesting, not only as a check on the radiative processes, but because of the relation of the turbulent damping to the excitation. Ulrich's observations show, for given wave-number, peaks at the expected normal mode frequencies. The widths of these peaks are uncertain because of the noise level, but it seems likely that it is due entirely to the spread of wavenumbers. Over the range from  $L = 10$  to  $L = 1500$ , the frequency of the lowest mode at given  $L$  varies very closely as  $L^{1/2}$ . Thus the expected frequency spread is  $\delta\omega/\omega = \frac{1}{2}\delta k/k$ . The calculations indicate that the turbulent damping increases with the wave number  $k$ . At  $L = 200$  and  $300$  the highest dissipation occurs in the modes with several radial nodes, but at  $L = 1000$  it decreases with increasing frequency. For the  $L = 1000$  fundamental mode the "natural" width  $\delta\omega/\omega = 3 \times 10^{-3}$  if the convective velocity has its usual value, and is about 10 times larger if the velocity is scaled up by a factor of 2. The spatial resolution required to see the latter value is possibly within reach of ground based observations if guiding problems can be minimized and the seeing is very good.

The problem of mode widths is discussed from a different viewpoint in the next section.

#### IV Are the Oscillations Really Global?

Do the solar oscillations know that they exist in a spherical body? If so, then the spectrum of horizontal wave numbers is discrete, and

power in the  $k - \omega$  plane should be found at distinct points rather than along continuous lines.

The radial modes, the gravity wave modes, and the p modes with low horizontal wave number, all have appreciable amplitude deep down in the sun, and thus are expected to be "global" modes. However, the p modes with spherical harmonic index  $L > 200$  are confined to a relatively thin surface layer comprising only 5% of the radius. The gross properties of these modes can be described quite adequately in a plane-parallel geometry, such as Ulrich's trapped wave model. Do these modes know they are in a spherical shell rather than an infinite plane slab? Physically, the question is closely related to whether an initially-localized disturbance can propagate far enough in space and time to see the spherical geometry. If the damping time of a normal mode is  $\gamma^{-1}$ , it might be expected that if  $c\gamma^{-1} > \text{circumference of the sun}$ , the mode would be aware of the shape. However, the usual soundspeed may be far from the correct number to use in this relation. In the present case, the dispersion relation is known to have the behavior  $\omega \propto k^{1/2}$  in the range of interest. Thus  $2\Delta\omega/\omega = \Delta k/k = \Delta L/L$ . If the mode width  $\Delta\omega$  is greater than  $\omega/(2L)$ , the dispersion relation allows a spread in wave number corresponding to one unit in  $L$ . This is the damping required for the wave-number spectrum to be continuous. This gives as the condition for discrete modes,

$$\gamma < 3.15 \times 10^{-4} L^{-1/2}$$

For  $L = 300$  the condition is  $\gamma < 1.82 \times 10^{-5}$ . This is less than a factor of two above the turbulent damping width for the 5 minute mode at  $L = 300$ , when the usual convective velocity is used. Since the turbulent damping increases with  $L$ , this condition is likely to be violated somewhere in the range  $L = 300$  to  $L = 1000$ .

Actually checking the discreteness of the 5 minute modes would be a difficult task. The individual modes sit in boxes with dimensions  $\delta k/k = L^{-1}$ ,  $\delta \omega/\omega = (2L)^{-1}$  in the  $k$ - $\omega$  plane. One or the other of these resolutions must be achieved if the question is to be decided. For periods in the range 3 minutes to 10 minutes, more than a day of observing time is required for this time resolution at  $L = 300$ . The spatial resolution is also difficult to reach. If the actual damping is higher than the estimate above, the transition from a discrete to a continuous wave number spectrum will occur at lower  $L$  where the time resolution problem is less severe.

#### V. Summary of Conclusions

1) It seems rather unlikely that low  $L$  p-modes can be responsible for the observed periods in the range 30-60 minutes. For g modes with  $L \leq 50$  the current calculations also fail to show a significant contribution by incoming waves to the adiabatic temperature perturbation near the temperature minimum. There are still some loopholes in the theory, and it is not known whether they can make a significant difference.

2) The stochastic excitation model for the 5 minute oscillations, while very crude, is capable of giving a total excitation energy comparable to that which is observed, without much need to adjust possible parameters in the theory. The calculations at present do not give a prediction of the high-frequency end of the spectrum because of the uncertainty in radiative damping rates.

3) It seems fairly likely that the global oscillation model is not strictly applicable to the high wave-number modes involved in the 5 minute oscillations.

## REFERENCES

Ando, H., and Osaki, Y. 1975, Publ. Astr. Soc. Japan, 27, 581.

Goldreich, P., and Keeley, D.A. 1977, Ap. J., 212, 243.

Hill, H.A., Stebbins, R.T., and Brown, T.M. 1976, Atomic Masses and Fundamental Constants, 5 ed. J.H. Sanders and A.H. Wapstra, (New York, Plenum), 622.

Hill, H.A., Caudell, T.P., and Rosenwald, R.D., in a paper presented at the Solar and Stellar Pulsation Conference, Los Alamos Scientific Laboratory, August 3-5, 1976.

Ulrich, R.K., and Rhodes, E.J. 1976. Preprint.

FIGURE CAPTION 1) The fractional temperature perturbation as a function of optical depth. The fractional displacement perturbation is essentially unity over the entire range, and its phase angle is zero degrees. The phase of the temperature perturbation relative to the displacement is indicated at several points along the curve.

FIGURE CAPTION 2) The wave-numbers  $k^{\pm}$  as a function of scale height ( $Y \equiv 2H$ ) for radial modes. The curve  $Y^{-1}$  lies halfway between the  $k^{+}$  and  $k^{-}$  curves.

FIGURE CAPTION 3) The wave numbers  $k^{\pm}$  as a function of scale height, for non-radial modes with horizontal wave number  $k_h$ .

FIGURE CAPTION 4) The excitation energy of the lowest frequency p mode as a function of the spherical harmonic number  $L$ . Results are shown for mixing-length/scale height = 1, and = 2, and for two choices of the convective velocity scale factor. A scale factor 1 corresponds to the ordinary mixing-length velocity.

FIGURE CAPTION 5) The excitation energy as a function of frequency for the modes between about 3 and 10 minutes for  $L = 300$ . The plotted symbols denote discrete normal modes.

FIGURE CAPTIONS 6 and 7) The (surface velocity)<sup>2</sup> predicted for the normal modes at  $L = 200$  and  $L = 300$ .

FIGURE CAPTIONS 8 and 9) The (surface velocity)<sup>2</sup> as a function of frequency and wave number, for two different mixing lengths.

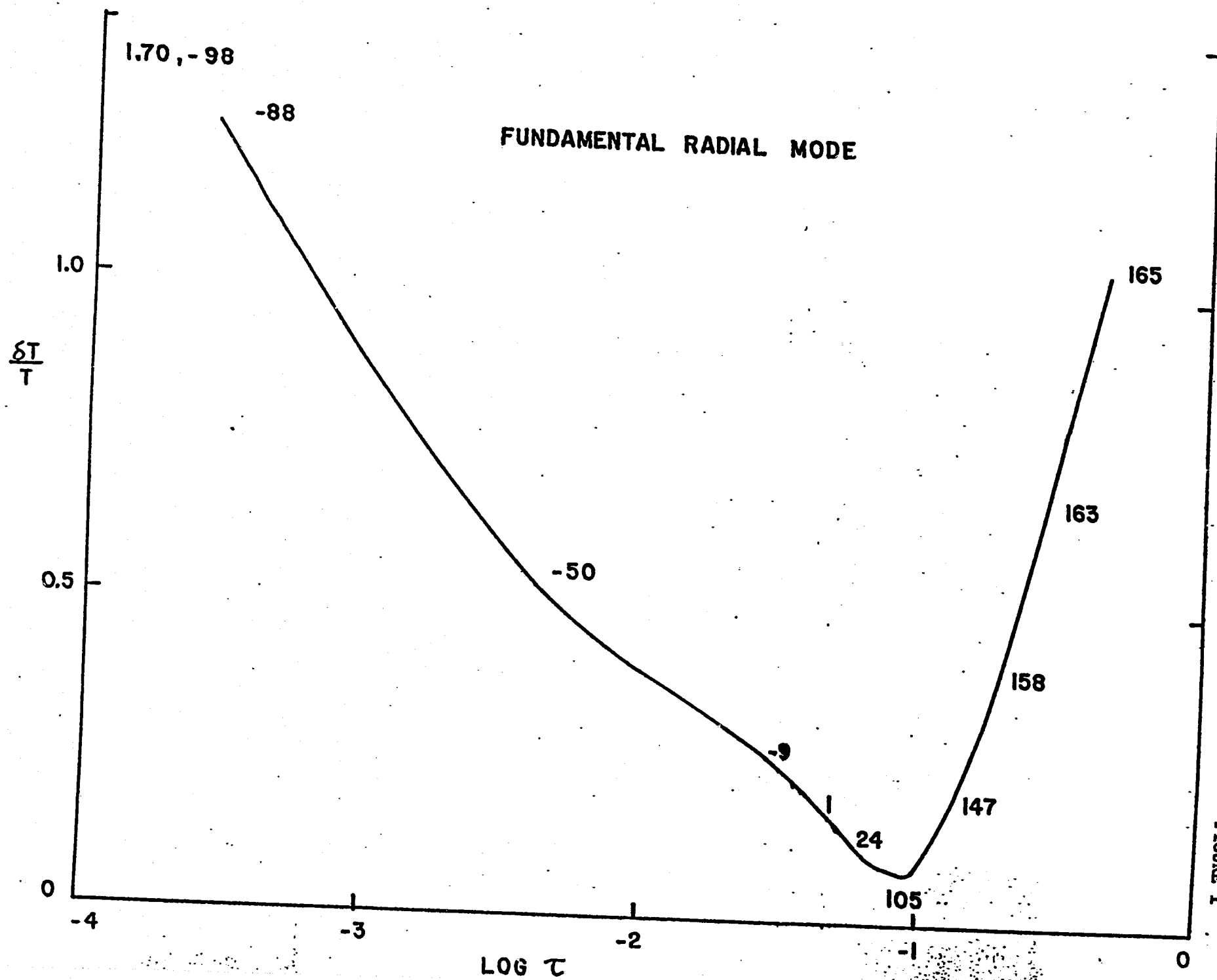


FIGURE 1

FIGURE 2

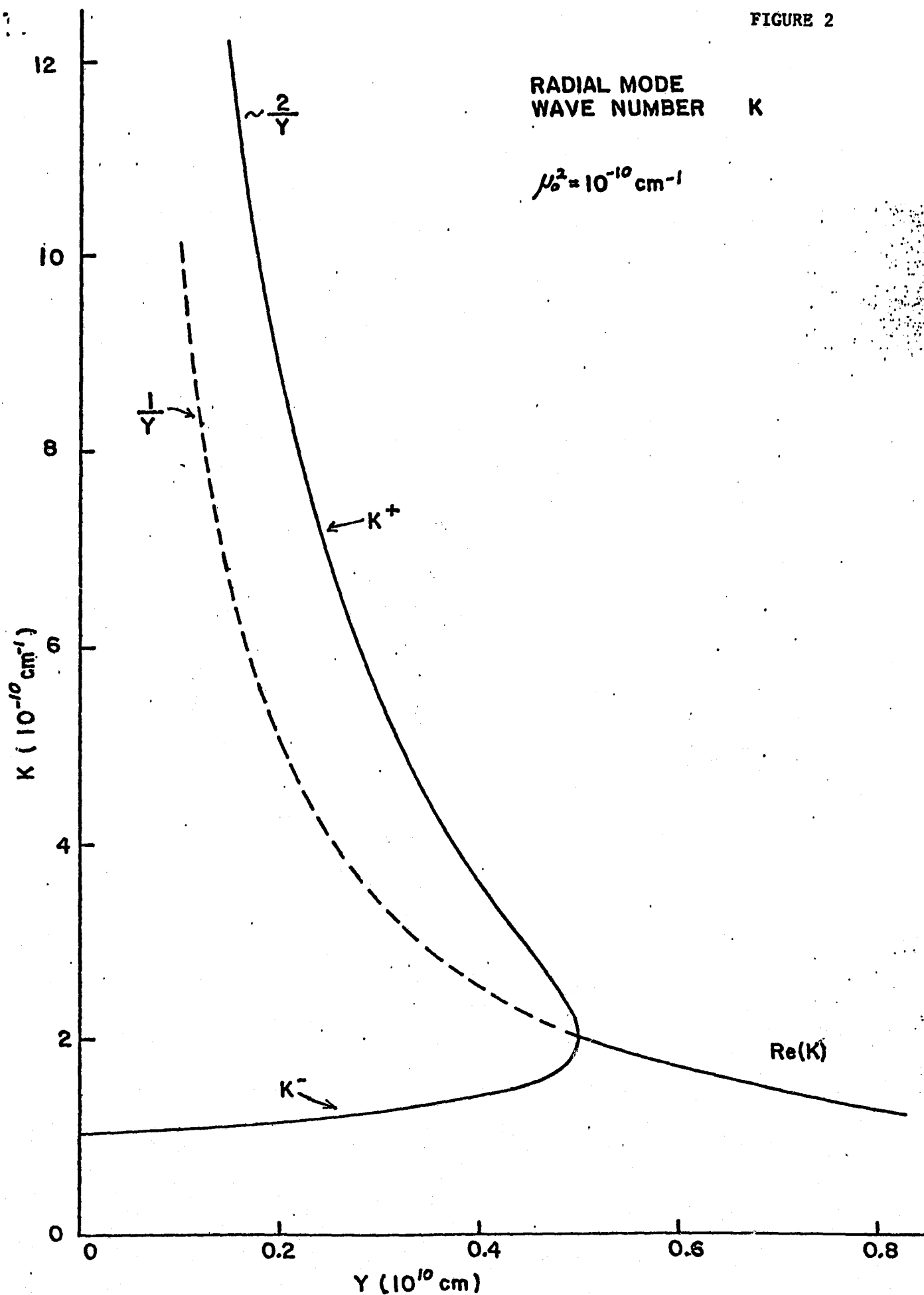




FIGURE 3

NON-RADIAL MODES

WAVE-NUMBER K

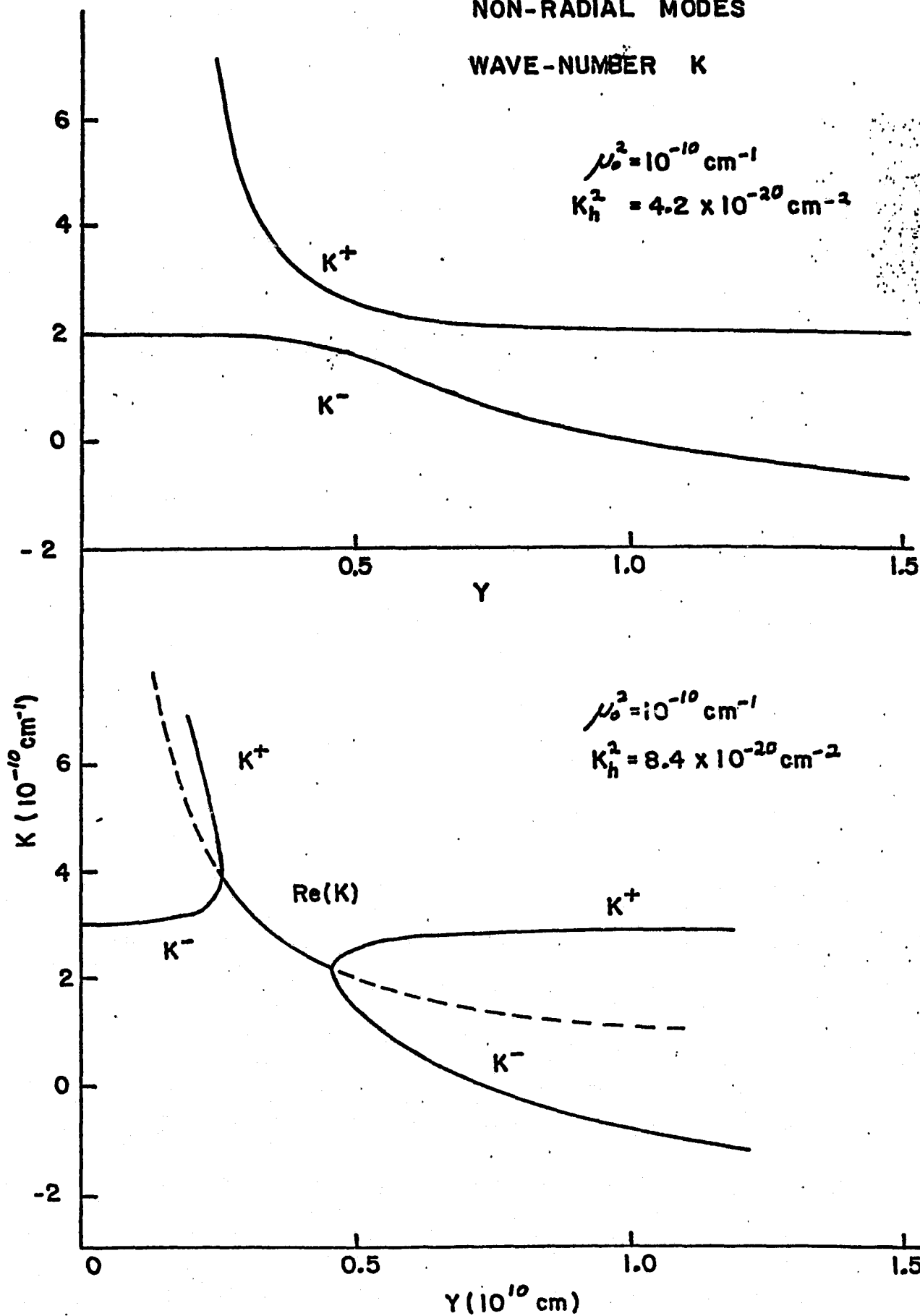


FIGURE 4

EXCITATION ENERGY OF LOWEST MODE

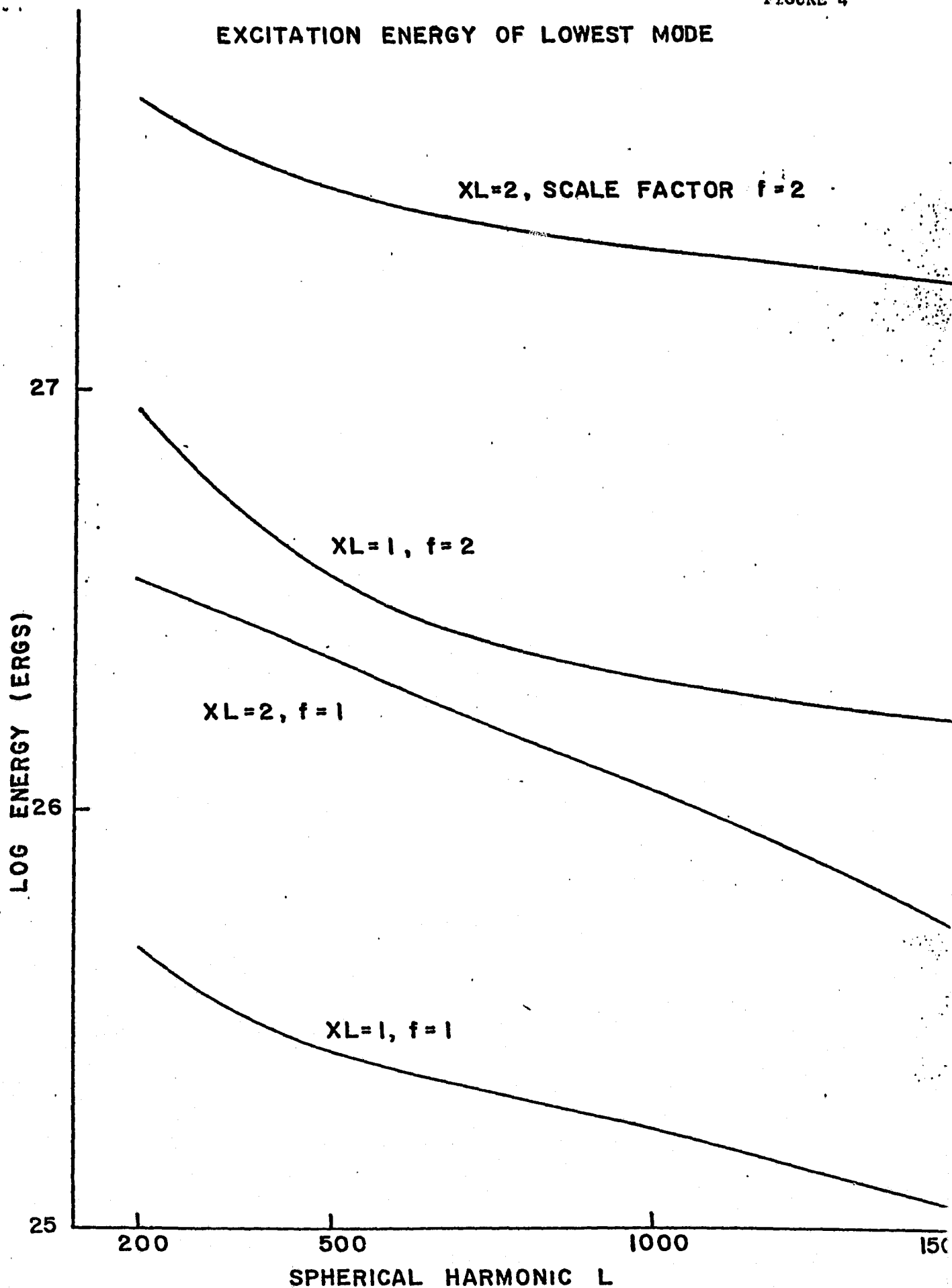


FIGURE 5

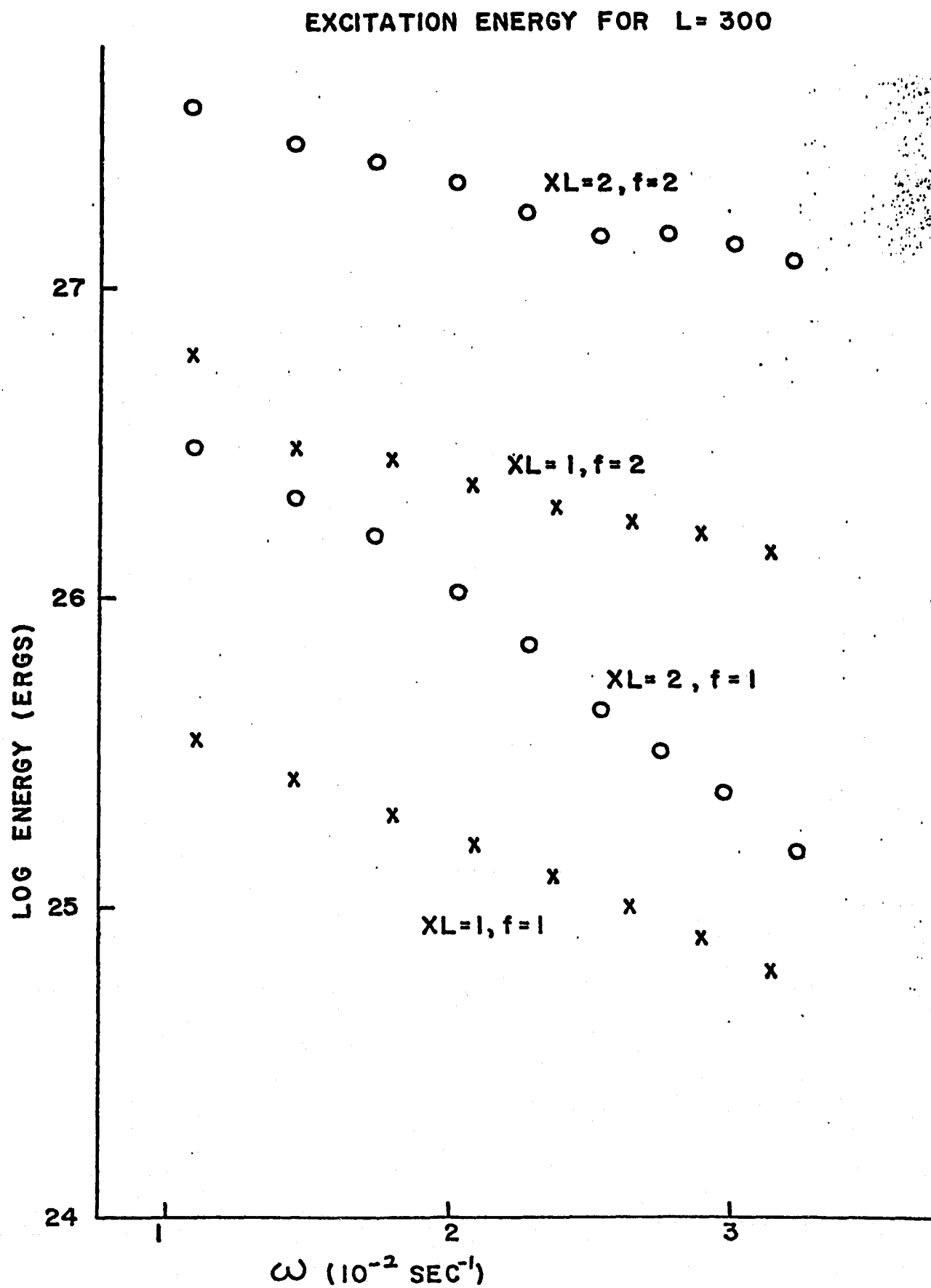


FIGURE 6

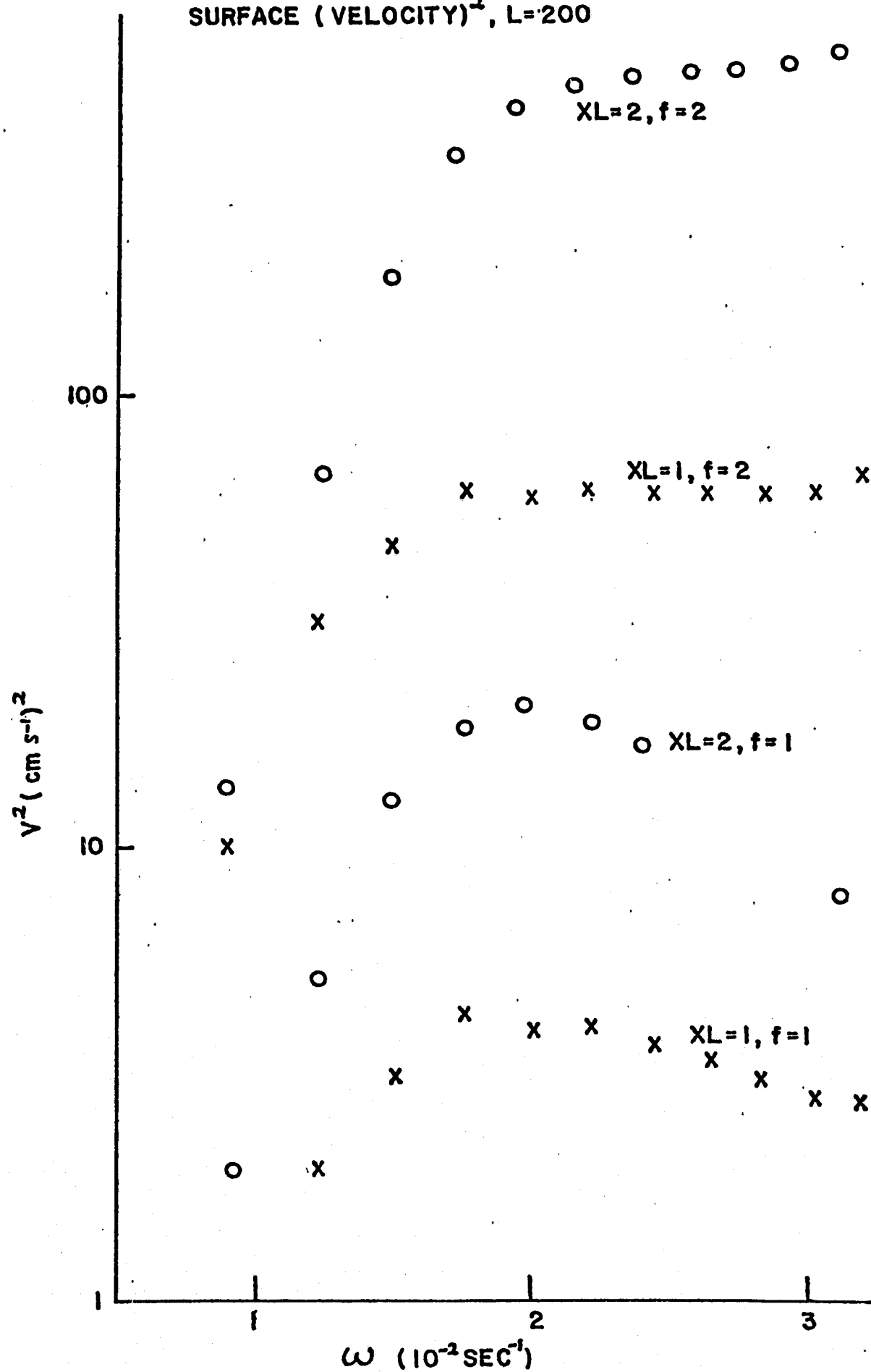
SURFACE (VELOCITY)<sup>2</sup>, L=200

FIGURE 7

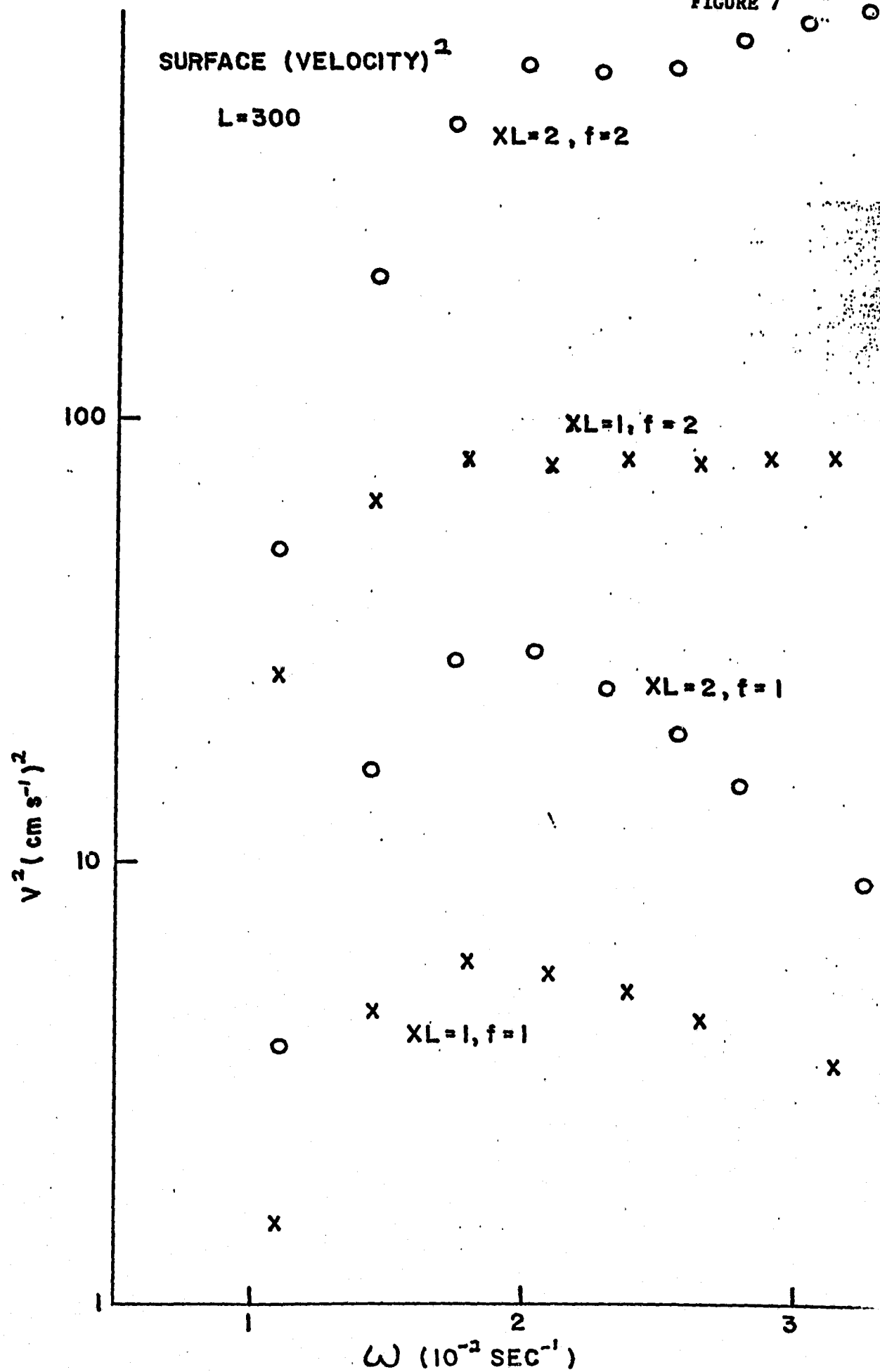


FIGURE 8

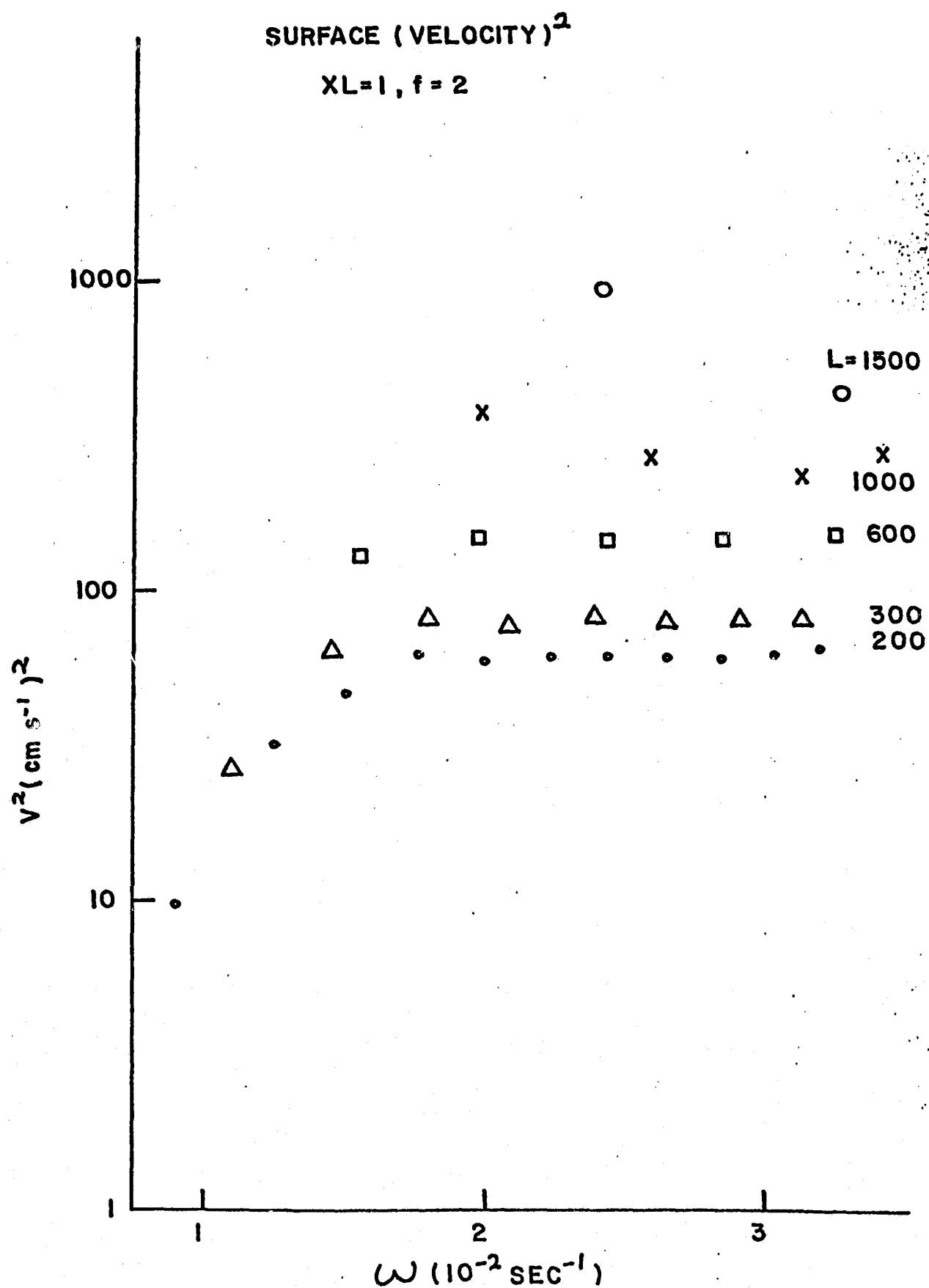
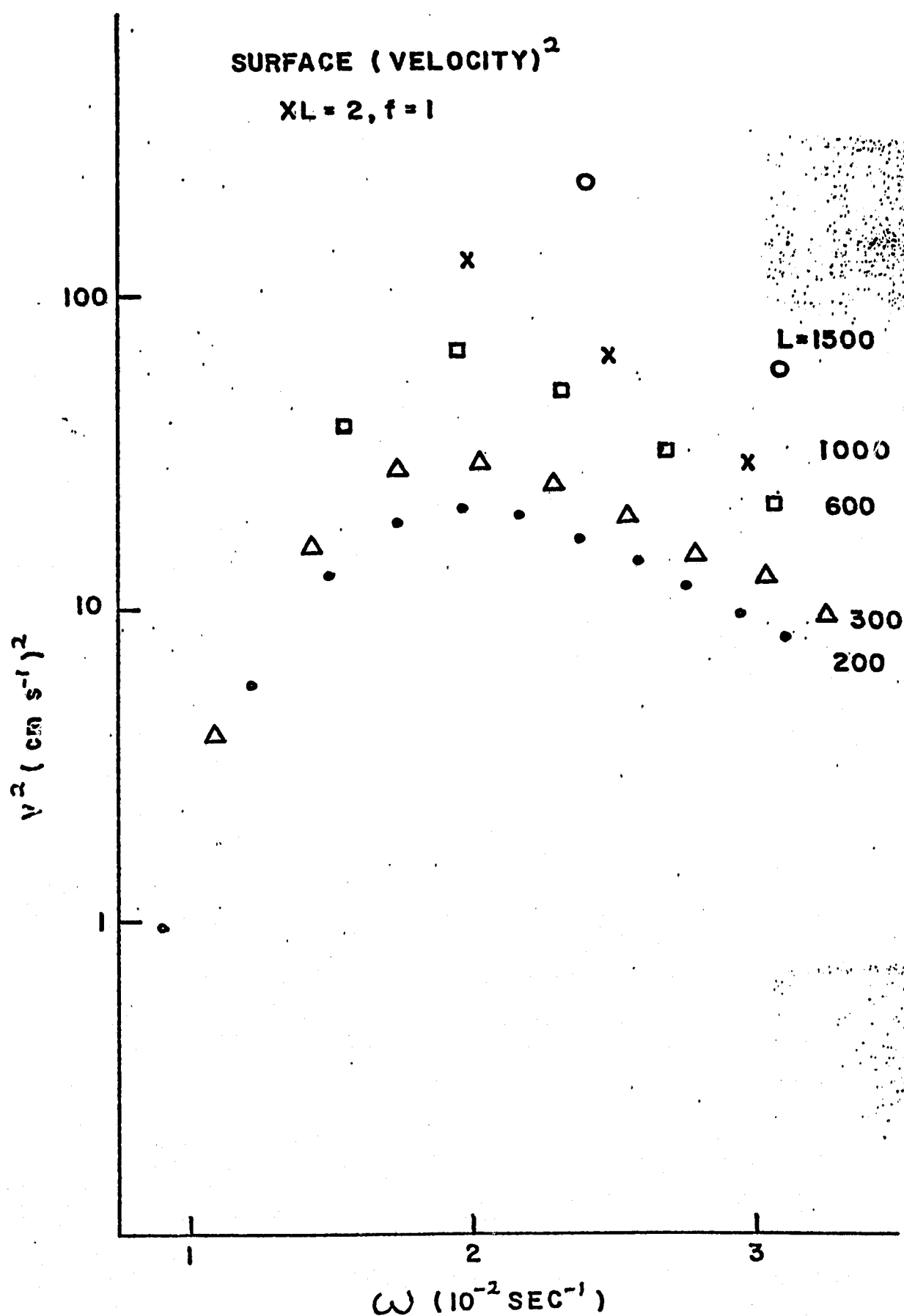


FIGURE 9



**A PRELIMINARY ATTEMPT TO INTERPRET THE POWER SPECTRUM OF THE  
SOLAR FIVE MINUTE OSCILLATIONS IN TERMS OF THE GLOBAL OSCILLATION MODEL.**

**D.A.Keeley**

**Lick Observatory, Board of Studies in Astronomy and Astrophysics  
University of California, Santa Cruz**

**To be presented at the Conference on Current Problems in Stellar  
Pulsation Instabilities, Goddard Space Flight Center, Greenbelt, Maryland  
June 1-2, 1978.**



# **ABSTRACT**

The observed power spectrum of the solar five minute oscillations is discussed from the viewpoint that the oscillations are excited by turbulent convection. The observations place significant constraints on the theory, and suggest constraints on the solar model structure.

## I. INTRODUCTION

The solar five minute oscillations provide a sensitive probe of the properties of the solar atmosphere and upper convection zone, and a challenge to theories which attempt to explain the amplitude of the oscillations as a function of frequency and spatial wave number. This paper discusses some properties of the power spectrum of the oscillations, in the context of the specific excitation mechanism described by Goldreich and Keeley (1977). It also discusses the effect of the atmospheric temperature profile, and the mechanical boundary condition. In §III the observed power spectrum as a function of aperture size is used to suggest constraints on the theoretical surface velocity of individual normal modes having periods near five minutes. It has already been noted by Ulrich and Rhodes (1977), that the frequency spectrum is better represented by solar models with mixing length equal to two or three pressure scale heights. It is shown in §IV that the steep low frequency side of the peak in the power spectrum is also more readily explained if the mixing length is greater than one scale height. The high frequency end of the power spectrum is also discussed.

## II. BRIEF DESCRIPTION OF OBSERVATIONAL DATA

The main observational data to be considered here are the shape of the power spectrum, and the dependence of the power density at a given frequency, on the horizontal scale observed. Examples of the data available are given by Fossat and Ricord (1975), and Fossat, Grec, and Slaughter (1977). For observations through circular apertures, the power spectrum shows a rather sharp peak very near 5 minute period, and the position and shape are rather insensitive to aperture diameter over the range from 22" up to

several minutes of arc. One of the most striking features is the steep rise on the low frequency side of the peak; the power density increases by a factor of about 6.5 between about 7 minutes and 5 minutes. On the high frequency side, the drop-off is roughly half as steep. An additional piece of information is the fall-off in power density at the peak, as a function of aperture size. The data of Fossat and Ricord (1975) suggest a drop by a factor  $\sim 2.5$  in power density, when the aperture diameter goes from 22" to 60".

### III. THE RELATIVE CONTRIBUTION OF DIFFERENT SPHERICAL HARMONIC MODES

#### a) Theoretical result of the averaging process.

Consider observations made through a circular aperture sufficiently small that the region viewed on the solar surface subtends a small solid angle at the center of the sun. Then the sphericity of the surface can be neglected and the vertical component of velocity can be written in the form

$$V(\theta, \phi, t) = \sum_{Lm} v_{Lm} Y_{Lm}(\theta, \phi) e^{-i\omega_{Lm}t},$$

in which  $\theta$  and  $\phi$  are spherical polar coordinate angles,  $Y_{Lm}$  is a spherical harmonic, and  $\omega$  is the oscillation frequency.  $v_{Lm}$  is the velocity amplitude for a given  $Lm$  mode. The spatial averaging can be carried out most simply if the polar axis of the coordinates is chosen to be the line of sight. Let  $\theta_0$  be the angular radius of the disc as seen from the center of the sun. Then

$$\begin{aligned} V &= \sum_{Lm} v_{Lm} e^{-i\omega_{Lm}t} \frac{1}{\Delta\Omega} \int_{\cos\theta_0}^1 Y_{Lm} d\Omega \\ &= \sum_L v_{L0} e^{-i\omega_{L0}t} \frac{2\pi}{\Delta\Omega} \left( \frac{2L+1}{4\pi} \right)^{\frac{1}{2}} \sin\theta_0 P_L^{-1}(\cos\theta_0), \end{aligned}$$

where  $P_L^{-1}$  is an associated Legendre function. For  $L\theta_0 \ll 1$ , but  $\theta_0 \ll 1$

$$v = \sum_L v_{L0} e^{-i\omega_{L0} t} \left( \frac{2L+1}{4\pi} \right)^{\frac{1}{2}}$$

and for  $L\theta_0 \gg 1$ , but  $\theta_0 \ll 1$ ,

$$v = \sum_L v_L \left( \frac{2}{\pi \theta_0^2} \right) \left( \frac{1}{L\theta_0} \right) \cos \left[ \left( L + \frac{1}{2} \right) \theta_0 - \frac{3\pi}{4} \right]$$

The theoretical calculations give mean square velocities for each normal mode; these are assumed to add incoherently. Thus the formulae above yield

$$v^2 = \sum_L v_L^2 \left( \frac{2L+1}{4\pi} \right), \quad L\theta_0 \ll 1, \text{ and}$$

$$v^2 = \sum_L v_L^2 \frac{4}{\pi^2 \theta_0^2} \frac{1}{(L\theta_0)^2} \cos^2 \left[ \left( L + \frac{1}{2} \right) \theta_0 - \frac{3\pi}{4} \right], \quad L\theta_0 \gg 1.$$

To compare with observations made with a finite bandwidth  $\Delta\omega$ , the sum over  $L$ 's is taken for all modes having frequencies within that band. If  $\Delta\omega$  is not too small, there will be one or more modes with no radial nodes, one or more with one radial node, one or more with two radial nodes, etc., contributing. Within each such group the  $L$  value will vary over a range depending on the bandwidth  $\Delta\omega$ , and the  $L$  values involved in different groups will be quite different except when  $L$  itself is small or the bandwidth is wide. From the calculated relation between frequency and  $L$  for modes with a fixed number of radial nodes,  $\frac{\Delta L}{L} \approx 2 \frac{\Delta\omega}{\omega}$ . Thus the number of modes expected in  $\Delta\omega$  is  $\sim 2 L \frac{\Delta\omega}{\omega}$ , provided this number is greater than unity;

if the bandwidth is very small some groups may not contribute at all. In this case, the bandwidth of the individual normal modes may be important. If within each group it is assumed that  $V_L^2$  is the same, the power can then be written as

$$V^2 = \frac{\Delta\omega}{\omega} \sum_L V_L^2 \left(\frac{2L+1}{4\pi}\right) (2L), L\theta_0 \ll 1$$

$$V^2 = \frac{\Delta\omega}{\omega} \sum_L V_L^2 \frac{4}{\pi^2 \theta_0} \frac{1}{(L\theta_0)^2} (2L) \cos^2\left[\left(L+\frac{1}{2}\right)\theta_0 - \frac{3\pi}{4}\right], L\theta_0 \gg 1.$$

where the sum now is over the central  $L$  values of each group. The power per unit frequency interval follows directly from these formulae.

#### b) Trial distributions of $V_L^2$

It is instructive to plug in some trial distributions for  $V_L^2$  as a function of  $L$ , to see whether any clues to the actual distribution of mode energies in the sun can be obtained. The  $L$  values for the groups depend on  $\omega$ ; for definiteness, a frequency  $\omega = 2 \times 10^{-2} \text{ sec}^{-1}$  was chosen. Approximate  $L$  values for groups near this frequency are as follows, for a model with mixing-length equal to one pressure scale height: 1004, 620, 386, 270, 195, 150, 120, 98, 80, 68, 56, 50, 43, 36, 30, 25, 19. Relative power densities were calculated corresponding to the following three cases: Case 1)  $V_L^2 = 1$  for all  $L$ . Case 2)  $V_L^2 = L$ . Case 3)  $V_L^2 = L^{-1}$ . The calculations were simplified by omitting the  $\cos^2$  factor, and by using the asymptotic form for small  $L\theta_0$  up to the point where it intersected the form for large  $L\theta_0$ . This occurred at  $L\theta_0 \approx 2\pi^{\frac{1}{3}}$ . The results are shown for six different aperture sizes, in table 2. The most important point to note is that in all three cases, the ratio of power densities at 22" and 60" is greater than the observed ratio of 2.5 noted earlier. Although these

calculations are extremely crude, they suggest that there may be problems if  $v_L^2$  is constant or an increasing function of  $L$ . In fact, current calculations (Keeley 1977) suggest that  $v_L^2$  increases with  $L$  for periods longer than  $\sim 3.5$  minutes, if turbulence provides the only damping mechanism. This suggests that it will be worthwhile to repeat the calculations presented in table 1, using an accurate representation of the Legendre function. Results similar to those of the crude calculation may present a severe challenge to the turbulent excitation theory, and a significant constraint on any theory which predicts amplitudes of individual normal modes. If, on the other hand, the observations at 22" suffer from seeing or guiding effects which reduce the power observed at high spatial wave number, then the results may be compatible.

#### IV. THE SHAPE OF THE POWER SPECTRUM

Since the observations suggest that the shape is relatively independent of aperture size, it is convenient to discuss the power spectrum corresponding to fixed values of  $L$ . Results for  $L = 100, 200$ , and  $300$ , all of which contribute to the power at periods as long as about 10 minutes, are considered in detail below. The discussion naturally divides into consideration of the energy to which an individual mode is excited, and the shape of the eigenfunction for the velocity amplitude. Of course, these are not totally independent, but this separation will be useful.

The preliminary results reported by Keeley (1977) showed that for models with mixing length equal to one or two pressure scale heights, the surface (velocity)<sup>2</sup> for  $200 \leq L \leq 600$  had a peak near  $\omega \approx 2 \times 10^{-2}$  (period  $\sim 5.25$  minutes). The peak was steepest on the low frequency side, in general agreement with observations. However, it was noted at that time

that the peak was not nearly sharp enough. These calculations include only turbulent dissipation in the calculation of the excitation energy, and the eigenfunctions were calculated for the adiabatic case.

a) The shape of the eigenfunctions

It is convenient to define an effective mass as the excitation energy required to produce a  $v^2$  (averaged over the surface, and in time) of  $(1 \text{ cm/sec})^2$ , at any particular depth in the atmosphere. This depends on the shape of the eigenfunction, but not on the actual excitation energy. The actual  $v^2$  is obtained as the quotient of the excitation energy and the effective mass.

On the low frequency side of the peak, the increase in  $v^2$  is due to an initial decrease in effective mass as the number of radial nodes in the eigenfunction increases. Physically, this occurs because the kinetic energy of the higher modes is more concentrated in the surface region, where the density is lower, and less energy is required to produce a given velocity. In the models discussed by Keeley, the excitation energy decreased with  $\omega$ , but this effect was more than compensated by the decrease in effective mass, for  $\omega < 2 \times 10^{-2}$ . At higher frequencies (in a sequence with fixed  $L$ ) the effective mass dropped off relatively slowly, and the net result was the high-frequency cut-off noted above.

The problem of insufficient steepness at low frequency can be approached from two directions. The first is to construct models in which the fall-off of effective mass is more rapid in the frequency range  $\omega = 1.5 \times 10^{-2}$  to  $2 \times 10^{-2}$ , and the second is to find models in which the excitation energy decreases more slowly with  $\omega$ , at least for periods greater than about 5 minutes. The latter problem is discussed in b) below. The ratio of

effective masses over a given frequency range is conveniently expressed as  $-\log(m(\omega_2)/m(\omega_1))/\log(\frac{\omega_2}{\omega_1})$ . In table 2 this ratio is shown for solar models with three different values of the mixing length. The eigenfrequencies are not the same in these three cases, but  $\omega_1 \approx 1.5 \times 10^{-2}$  and  $\omega_2 \approx 2 \times 10^{-2}$  for the functions chosen. It is clear from the table that the model with largest mixing length is the most favorable, at all  $L$  values considered. If the excitation energies were roughly equal over this frequency range, the slope would be almost steep enough. Of course, the exact comparison with observations through a circular aperture requires that the results for various  $L$  values be combined as discussed in §III above. The results shown in table 2 are for models which have a fairly realistic atmosphere out to a temperature minimum of 4180°K.

Some preliminary calculations of nonadiabatic eigenfunctions have also been done. Including turbulent viscosity in the equations of motion does not have a significant effect on the shape of the eigenfunction, as reflected in the effective masses for the low frequency, low  $L$  modes studied so far. On the other hand, a fully nonadiabatic treatment of the radiative dissipation has a significant effect, apparently because the dissipation is very strongly localized near the top of the convection zone. For the cases studied, the result is to steepen the decrease in effective masses with increasing frequency, and thus to steepen the low-frequency side of the peak of the power spectrum. The nonadiabatic calculations can't at present be done correctly with a realistic solar atmosphere, since the radiation flux is not given simply in terms of the temperature gradient, as in the approximation usually used for stellar interiors. Also, the effects of convection are not included.



i) Effect of surface temperature and the mechanical boundary condition.

Models computed using the diffusion approximation all the way to the surface had surface temperatures of about  $4880^\circ$ . A more realistic value of  $T$  at the temperature minimum is about  $4180^\circ$  (Allen 1976). Adiabatic eigenfunctions and frequencies were computed for the diffusion models, and for models in which the empirical temperature profile was used at the surface. In addition, the models were computed with two different boundary conditions, one being that the Lagrangian pressure perturbation vanish at the surface, and the other that an outgoing wave existed (evanescent or propagating) with radial wave number determined as if the surface had an isothermal region attached to it at the boundary point of the model. The effect of a lower temperature at the surface is to make the waves more evanescent, and is expected to be most important at high frequency. At periods  $\lesssim 5$  minutes, it was found that with the  $\delta^L P = 0$  boundary condition the low  $T$  model had lower effective masses (at optical depth  $10^{-3}$ ) and a slightly steeper decline in effective masses with increasing  $\omega$  than the high surface temperature model. With the outgoing wave condition the situation was the opposite for both the magnitude of the effective mass, and the ratios of effective masses. In general, for either surface temperature, models with the outgoing wave condition had lower effective masses. The differences were largest at the highest frequency, where the waves were closest to being able to propagate. Significant changes in eigenfrequencies occurred only when the modes were close to propagating. Otherwise, the two atmosphere models and two boundary conditions gave nearly equal frequencies for the same physical oscillation modes.

## b) The Excitation Energy

In the theory described by Goldreich and Keeley (1977), the expression for the excitation energy of a normal mode is given in the form of a quotient of two numbers. The denominator is the damping rate of the normal mode, and the numerator is a double integral, over depth in the model, and over eddy sizes at a given depth. An improved approximation to the inner integral has been used in the calculations described here.

### i) Low frequency behaviour

In the discussion of the low frequency side of the peak in the power spectrum, it was noted that if the excitation energies over that frequency range were roughly equal, then the steep decline in effective mass for the high mixing-length models produced a slope much more in line with the observations. However, for all three mixing lengths tested, the excitation energy decreased significantly with increasing frequency. One way of equalizing the excitation energies for periods greater than about 5 minutes is to make all modes derive the main contribution to their excitation energy from a single set of eddies. The desired result will then be expected, provided the equipartition argument (Goldreich and Keeley 1977) is approximately valid. The result can be achieved, in fact, by a decrease in the correlation time for eddies in the outer part of the convection zone. If  $\omega \tau_c < 1$  at  $\omega \approx 2 \times 10^{-2}$  for the largest, most energetic eddies at a given depth, then all modes with  $\omega < 2 \times 10^{-2}$  will tend towards energy equipartition with these eddies. If  $\omega \tau_c > 1$  for the largest eddies, then the modes will tend to equipartition with a smaller, less energetic eddy having a correlation time satisfying  $\omega \tau \approx 1$ . In the present theory, the correlation time for the largest eddies is taken to be the mixing length divided by the convective velocity, and is scaled to

smaller eddies by assuming a Kolmogoroff spectrum. Then the integral over eddy sizes depends on the correlation time assumed for the largest eddies in the form

$$\mathcal{Q}(\omega) = \tau_c \int_0^1 \frac{dx}{x} x^{7.5} \exp\left(-\frac{1}{4} \omega^2 \tau_c^2 x^2\right)$$

This is a slow function of  $\omega$  for  $\omega \tau_c \ll 1$ , but drops like  $\omega^{-7.5}$  for  $\omega \tau_c \gg 1$ . The changeover between the two types of behaviour is rather gradual; thus a change in  $\tau_c$  which shifts the low frequency modes into the flat region results in a slower fall-off of the excitation energy, and therefore of the power spectrum, at high frequency.

The behaviour of excitation energy expected from the above discussion was verified by artificially increasing the convective velocity near the surface of the convection zone. A factor of less than two was sufficient to achieve the desired result. Thus it appears possible to reproduce, more or less, the steep rise in the power spectrum by a decrease in correlation time, in combination with a model with large mixing length. Of course, some of this gain is at the expense of the high-frequency fall-off.

## ii) High frequency behaviour

The power spectrum as presently computed does not fall off very fast at high frequencies, at fixed  $L$ , except for  $L > 1000$  or so (Keeley 1977). If such high  $L$  values do make substantial contribution to the power observed through typical apertures, they will improve the shape of the high frequency end substantially. However, it seems likely that radiative damping will play a significant role in decreasing the excitation energy

for high-frequency modes. The only published nonadiabatic results on radiative damping are those of Ando and Osaki (1975, 1977). They find that the modes around 5 minutes are linearly unstable, but that modes near 3 minutes are stable. Strong damping sets in at somewhat lower frequency in their 1977 calculations, which include a chromosphere and corona. For the present models, the turbulent damping exceeds the radiative driving in all cases, but they are comparable for some modes. The result of a negative contribution to the damping would be an increase in the excitation energy of those modes; this could have a significant effect on the spectrum. For periods greater than about 7 minutes, the radiative growth or decay rate is relatively small compared to the turbulent decay rate. One important source of uncertainty is the calculation of the damping by the turbulent viscosity approximation. In addition, the calculations by Ando and Osaki do not include convection, and also do not calculate the radiative flux perturbation strictly correctly in the part of their model which employs an empirical  $T(\tau)$  relation. Some preliminary nonadiabatic calculations using models with the high-temperature boundary, but no convective perturbations, find stability for all modes checked in the 3 to 10 minute range, without the effect of turbulent viscosity. A further source of uncertainty is the convective velocity profile (and magnitude) in the outer part of the convection zone, since this region contributes strongly to both the turbulent damping, and the total excitation.

## V. SUMMARY OF RESULTS

The crude calculation of the power density near five minute period, as a function of aperture size, is not in agreement with observations; if a more accurate calculation establishes this discrepancy more firmly, then the observations may provide a powerful constraint on any theory of the excitation of the oscillations. In the present state of the theory, it seems possible to explain the steep low frequency side of the power spectrum peak. This requires, however, that the mass distribution of the sun be more like that of a model with a mixing length of three pressure scale heights, than one scale height. Important uncertainties in the damping due to radiative and convective energy transport preclude any strong statements about the high frequency end of the power spectrum; if there is linear driving comparable to the turbulent damping for periods near five minutes, this could have a significant effect on the sharpness and position of the peak.

This work was supported in part by NASA grant NGL-05-002-003.

## REFERENCES

- Allen, C. W. 1976, Astrophysical Quantities, (Third edition, London: Athlone Press).
- Ando, H. and Osaki, Y. 1975, Publ. Astron. Soc. Japan, 27, 581.
- Ando, H. and Osaki, Y. 1977, Publ. Astron. Soc. Japan, 29, 221.
- Fossat, E., Grec, G., and Slaughter, C. 1977, Astron. and Astrophysics, 60, 151.
- Fossat, E. and Ricord, G. 1975, Astron. and Astrophys. 43, 243.
- Goldreich, P., and Keeley, D. 1977, Ap. J. 212, 243.
- Keeley, D. 1977. Proceedings of the Symposium on Large Scale Motions on the Sun, Sacramento Peak Observatory, Sept. 1-2, 1977.
- Ulrich, R. K., and Rhodes, E. J. 1977, Ap. J. 218, 521.

TABLE 1

Power density as a function of aperture size for three different assumptions about the velocities.

Case 1:  $v_L^2 = 1$

Case 2:  $v_L^2 = L$

Case 3:  $v_L^2 = L^{-1}$

Aperture diameter		<2"	5"	10"	22"	60"	120"
$\theta_0$		< .00135	.00325	.0065	.0143	.0390	.078
$L_c$		> 1004	418	209	95	35	17
Case 1	Power density $L < L_c$	$3.25 \times 10^6$	$4.66 \times 10^5$	$2.13 \times 10^5$	$4.38 \times 10^4$	$3.85 \times 10^3$	$\sim 0$
	Power density $L > L_c$	0	$3.87 \times 10^5$	$1.65 \times 10^5$	$6.83 \times 10^4$	$1.33 \times 10^4$	$3.02 \times 10^3$
	Total	$3.25 \times 10^6$	$8.53 \times 10^5$	$3.78 \times 10^5$	$1.12 \times 10^5$	$1.72 \times 10^4$	$3.02 \times 10^3$
Case 2	Power density $L < L_c$	$2.69 \times 10^9$	$1.84 \times 10^8$	$2.97 \times 10^7$	$2.63 \times 10^6$	$1.01 \times 10^5$	$\sim 0$
	Power density $L > L_c$	0	$2.96 \times 10^8$	$7.40 \times 10^7$	$1.39 \times 10^7$	$1.20 \times 10^6$	$\sim 1.82 \times 10^5$
	Total	$2.69 \times 10^9$	$4.80 \times 10^8$	$1.03 \times 10^8$	$1.65 \times 10^7$	$1.30 \times 10^6$	$\sim 1.82 \times 10^5$
Case 3	Power density $L < L_c$	$6.52 \times 10^3$	$3.27 \times 10^3$	$1.95 \times 10^3$	$8.23 \times 10^2$	$1.51 \times 10^2$	$\sim 0$
	Power density $L > L_c$	0	$5.32 \times 10^2$	$4.45 \times 10^2$	$4.68 \times 10^2$	$2.29 \times 10^2$	$8.7 \times 10^1$
	Total	$6.52 \times 10^3$	$3.80 \times 10^3$	$2.40 \times 10^3$	$1.29 \times 10^3$	$3.80 \times 10^2$	$8.7 \times 10^1$

TABLE 2

Logarithmic slope  $\frac{\Delta \log (\text{effective mass})}{\Delta \log (\omega)}$  between  $\omega \approx 1.5 \times 10^{-2}$  and  $\omega \approx 2 \times 10^{-2}$ ,  
at three optical depths, for three values of mixing length/pressure scale height.

Mixing length		1	2	3
L = 100	$\tau = 10^{-3}$	2.596	4.306	4.944
	$\tau = 10^{-2}$	2.087	3.929	4.563
	$\tau = 0.7$	1.213	3.072	3.688
L = 200	$\tau = 10^{-3}$	2.846	4.491	5.060
	$\tau = 10^{-2}$	2.426	4.150	4.719
	$\tau = 0.7$	1.561	3.378	3.949
L = 300	$\tau = 10^{-3}$	2.756	4.746	5.337
	$\tau = 10^{-2}$	2.323	4.419	5.011
	$\tau = 0.7$	1.517	3.676	4.271



## EXCITATION OF SOLAR G MODES WITH PERIODS NEAR 160 MINUTES

D. Keeley  
Science Applications, Inc.  
Palo Alto, California

### ABSTRACT

Solar g modes with  $n = 1$  to 4 and periods near 160 minutes have been investigated using a solar model with normal structure. Radiative dissipation in the region below the convection zone is much greater than the driving provided by nuclear reactions or the opacity mechanism. A crude treatment of convection suggests that it also is not an important source of driving. The damping due to turbulent viscosity is also small. Excitation of these modes by coupling to convective turbulence is substantial in terms of the rms energy of the modes, but the surface velocity is very small because of the large amount of mass involved in the oscillation.

### 1. INTRODUCTION

The  $2^h 40^m$  period first reported by Severny, Kotov and Tsap (1976) and by Brookes, Isaak and van der Raay (1976) has been supported by more recent observations (Scherrer et al. 1979). In this paper, properties of modes in this period range are examined in the context of a conventional solar model, and their stability investigated as described below.

A model representing the sun was obtained by evolving a homogeneous  $1 M_{\odot}$  model from the zero age main sequence until it resembled closely the present sun. The properties of the model were as follows:  $L = 3.83 \times 10^{33}$  erg sec $^{-1}$ ,  $R = 6.9136 \times 10^{10}$  cm,  $Z = .02$ ,  $Y(\text{surface}) = .244$ ,  $X(\text{center}) = 0.59$ . The mixing length was 1.238 pressure scale heights. The convection zone included about  $1.2 \times 10^{31}$  grams and extended down to a temperature of about  $1.5 \times 10^6$  K.

The differential equations for adiabatic eigenfunctions were written in the form used by Osaki (1975), and solved by the method of inverse iteration. The damping (or excitation) was then determined by perturbation theory, using the adiabatic eigenfunctions. The turbulent excitation energy and viscous damping were calculated as described by Goldreich and Keeley (1977), except for an improvement in the integral over the wave numbers in the turbulent spectrum.

### 2. LINEAR STABILITY ANALYSIS

The condition for linear instability is that a net positive amount of PdV work be done during one cycle of the oscillation. In calculating growth rates according to perturbation theory, only the nonadiabatic part of the pressure perturbation can contribute to the work integral. If the time dependence is assumed

to be  $\exp(i\omega t)$ , then the nonadiabatic pressure perturbation is

$$\delta P_{na} = - \frac{(\Gamma_3 - 1)\rho}{i\omega} \delta \left( \frac{\nabla \cdot \vec{F}}{\rho} - \epsilon \right) \quad (1)$$

in which  $\delta$  denotes a Lagrangian perturbation, and all other symbols have their usual meaning. For a given mass element, there is a positive contribution to the driving if

$$\nabla \cdot \vec{\xi} \delta \left[ \frac{\nabla \cdot \vec{F}}{\rho} - \epsilon \right] > 0, \quad (2)$$

in which  $\vec{\xi}$  is the displacement.

### 2.1. Radiative Contribution

The equations used for the radiative flux  $\vec{F}_r$  are

$$\vec{F}_r = - \frac{4\pi}{3\kappa\rho} \nabla J \quad (3)$$

$$J - B = - \frac{1}{4\pi\kappa\rho} \nabla \cdot \vec{F}_r \quad (4)$$

in which  $J$  is the mean intensity,  $B$  is the Planck function, and  $\kappa$  is the absorption coefficient. Since the perturbation of the scalar quantity  $\nabla \cdot \vec{F}_r$  is required in equation (2), it is convenient to write an equation for it directly:

$$\nabla \cdot \vec{F}_r - \frac{1}{3} \nabla \cdot \left[ \frac{1}{\kappa\rho} \nabla \left( \frac{1}{\kappa\rho} \nabla \cdot \vec{F}_r \right) \right] = - \frac{4\pi}{3} \nabla \cdot \left( \frac{1}{\kappa\rho} \nabla B \right) \quad (5)$$

The second term on the left is usually omitted in calculations of both the hydrostatic model and the damping. Its effect on hydrostatic models is normally small, but for some oscillation modes its perturbations have a large effect on the damping. It is especially important at the outer boundary of the solar convection zone.

It is customary to do Eulerian perturbations in nonradial calculations because they commute with spatial derivatives; this problem is more difficult to deal with in these circumstances than it is for radial motions. However, in regions where  $\kappa$  or other quantities vary very rapidly in space, the Eulerian perturbations are very much larger than Lagrangian perturbations. Because it is ultimately necessary to construct the Lagrangian perturbation for use in equation (2), the cancellation of

several significant digits, which could result when going from Eulerian to Lagrangian at the outer edge of the convection zone, could have a serious effect. Numerical errors due to noise in the eigenfunctions could occur in this potentially important driving region. Even if the eigenfunctions are not noisy, possible systematic effects due to the grid structure could introduce significant errors. For these reasons, Lagrangian perturbations were used throughout, and terms which were cancelled in part or totally by similar terms from the convective flux perturbations were handled explicitly. The final expression for the perturbation of  $\nabla \cdot \vec{F}_r \equiv D$  is:

$$\begin{aligned} \delta D - \frac{1}{3} \left[ \beta (\delta \delta D); K \right]; K = & -\frac{4\pi}{3} \left[ \beta (\delta \delta B); K \right]; K + \frac{1}{3} \left[ \beta (\delta \delta D); K \right]; K \\ & + \left( \frac{\delta \beta}{\beta} F_{rK} \right); K - \left( \epsilon_{JK} F_{rJ} \right); K - \epsilon_{JK} F_{rK}; J \end{aligned} \quad (6)$$

in which  $\beta \equiv (\kappa \rho)^{-1}$ . Index notation has been used because ordinary vector notation is somewhat ambiguous for the last two terms. The semicolons denote covariant derivatives.

## 2.2. Convective Contribution

An equation for the time-dependent convective flux was written in the form given by Cox et al. (1966):

$$\frac{d\vec{F}_C}{dt} = \frac{\vec{F}_C^{(i)} - \vec{F}_C}{\tau}, \quad (7)$$

in which the timescale  $\tau$  is taken to be the mixing length divided by the local convective velocity, and  $\vec{F}_C^{(i)}$  is the convective flux as calculated from mixing length theory. The perturbed form of the equation is

$$\delta \vec{F}_C = \frac{\delta \vec{F}_C^{(i)}}{1 + i\omega\tau}. \quad (8)$$

The Lagrangian perturbation of the instantaneous flux was taken to be

$$\delta \vec{F}_C^{(i)} = \delta \left( -F_C^{(i)} \frac{\nabla P}{|\nabla P|} \right), \quad (9)$$

in which a unit vector in the direction of  $-\nabla P$  is taken as the direction of the convective flux, and  $F_C^{(i)}$  is the magnitude of the flux as calculated in the usual way. Equation (9) expands out to the form

$$\delta \vec{F}_C^{(1)} = \delta F_C^{(1)} \hat{r} - \frac{F_C^{(1)}}{r} \left( H \frac{\delta P}{P} - (\xi_l - \xi_r) \right) \nabla_l \cdot \nabla_{lm} , \quad (10)$$

in which  $H$  is the pressure scale height,

$$\nabla \equiv \hat{r} \frac{\partial}{\partial r} + \frac{1}{r} \nabla_l , \text{ and } \vec{\xi} = \xi_r \hat{r} \cdot \nabla_{lm} + \xi_l \nabla_l \cdot \nabla_{lm} .$$

The perturbation of the divergence of  $\vec{F}_C$  is given by

$$\delta(\nabla \cdot \vec{F}_C) = \nabla \cdot (\delta \vec{F}_C) - \nabla \vec{\xi} : \nabla \vec{F}_C , \quad (11)$$

in which the last term is the same form as in equation (6) for the radiative flux, and is partly cancelled by it.

### 2.3. Nuclear Contribution

The energy generation rate has been written in the usual form:

$$\epsilon = \epsilon_0 \rho^n T^\nu , \quad (12)$$

from which the perturbation in the adiabatic approximation is obtained:

$$\frac{\delta \epsilon}{\epsilon} = -\nabla \cdot \vec{\xi} [\eta + (\tau_3 - 1)\nu] . \quad (13)$$

Constant values for  $\eta$  and  $\nu$  were used throughout the energy-generating region. Since  $\tau_3 - 1$  is quite constant also, the nuclear contribution can easily be scaled to any desired values of the exponents  $\eta$  and  $\nu$ . For the results given in Table 1, the values  $\eta = 1$ ,  $\nu = 15$  were used. The high value for  $\nu$  was used because the nuclear reactions cannot maintain the equilibrium abundance of products in the PP chain for which the exponent  $\nu \sim 4$  or 5 is appropriate. Since nuclear driving did not appear to be an important effect, it was not considered necessary to treat this contribution in more detail.

### 2.4. The Condition for Local Driving

With the approximations discussed above, the condition for driving of the instability (equation 2) becomes

$$\nabla \cdot \vec{\xi} \left\{ \frac{\delta(\nabla \cdot \vec{F})}{\rho} + \nabla \cdot \vec{\xi} \epsilon + \epsilon \nabla \cdot \vec{\xi} [\eta + (\tau_3 - 1)\nu] \right\} > 0 . \quad (14)$$

The nuclear reactions always contribute to instability, as does the density perturbation in a region where  $\nabla \cdot \vec{\xi} > 0$ .

Table 1

TABLE 1. g Modes Near  $2h_{40}^m = 9600s$ 

$l =$	1	2	3	4
Period (s)	10196	9473	9840	9647
Nodes	6	10	15	19
Amplitude ratio	12	10	22	36
Radiative damping rate ( $s^{-1}$ )	1.40-13	4.02-13	9.16-13	1.49-12
Convective damping rate	8.80-17	-1.38-15	-4.26-15	-5.75-15
Turbulent damping rate	1.92-15	1.50-14	2.61-14	2.85-14
Nuclear excitation rate	1.29-14	1.33-14	1.37-14	1.38-14
Radiative damping below convection zone	99%	98%	96%	96%
Turbulent excitation energy (ergs)	9.3+25	1.6+26	1.3+26	7.9+25
Energy for 1 cm/sec at surface (ergs)	1.1+33	5.8+32	8.7+32	1.4+33

### 3. RESULTS AND CONCLUSIONS

Adiabatic eigenfunctions and frequencies were calculated for several modes at each value of  $\lambda$  in the range  $\lambda = 1$  to 4, and the work integral was calculated as described in § 2 above. The results are summarized in Table 1 for the 4 modes with periods closest to 160 minutes. In addition, the radial and transverse components of  $\xi$  are shown in Figure 1 for the  $\lambda = 1$  mode. The 200 point grid resolved the 6 nodes of the  $\lambda = 1$  mode quite well, but resolution was not as good for the 19 nodes at  $\lambda = 4$ . However, it is unlikely that errors large enough to alter the conclusions are present.

Except for the  $\lambda = 1$  mode, the ratio of the maximum radial displacement to the surface displacement increased strongly with  $\lambda$ , as indicated in Table 1. Radiative damping was by far the dominant dissipative mechanism, and most of that damping occurred below the convection zone. Convective flux transport provided driving near the surface of the convection zone in an amount comparable to the radiative driving there. The energy expected in these modes as a result of nonlinear coupling to convective turbulence was  $\sim 10^{26}$  ergs, whereas the energy required for a surface velocity of 1 cm/sec is  $\sim 10^{33}$  ergs. In any case, the turbulent excitation mechanism would not be a satisfactory one unless the observations eventually show that many modes are excited.

The observations are not easily understood in terms of the conventional considerations discussed in this paper.

### REFERENCES

- Brookes, J.R., Isaak, G.R. and van der Raay, H.B. 1976, *Nature*, 259, 92.  
 Cox, J.P., Cox, A.N., Olsen, K.H., King, D.S. and Eilers, D.D. 1966, *Ap. J.*, 144, 1038.  
 Goldreich, P. and Keeley, D.A. 1977, *Ap. J.*, 212, 243.  
 Osaki, Y. 1975, *Publ. Astron. Soc. Japan*, 27, 237.  
 Scherrer, P.H., Wilcox, J.M., Kotov, V.A., Severny, A.B. and Tsap, T.T. 1979, *Nature*, 277, 635.  
 Severny, A.B., Kotov, V.A. and Tsap, T.T. 1976, *Nature*, 259, 87.

ORIGINAL PAGE IS  
 OF POOR QUALITY

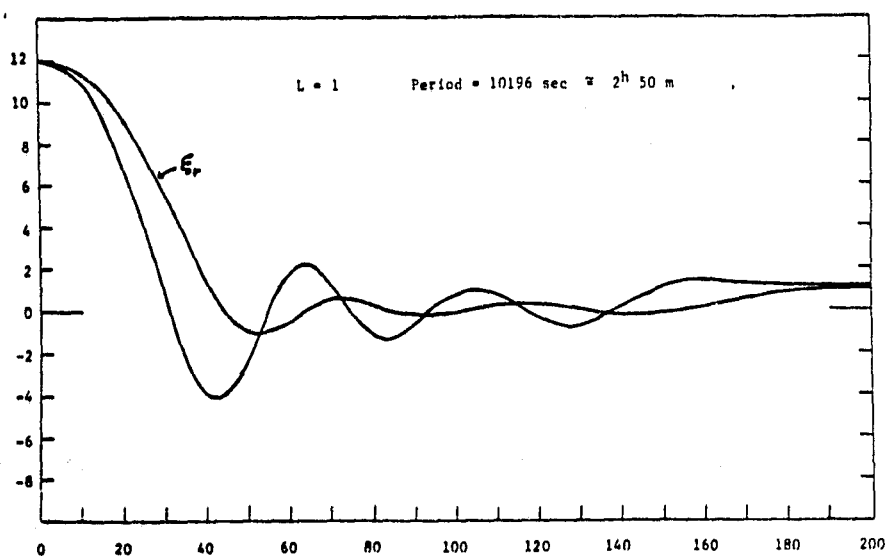


**Figure 1.** The radial and transverse components of the displacement vector for the  $l = 1$  mode. The eigenfunctions are normalized so that  $\epsilon_r = 1$  at the surface. The abscissa is the grid point number. The lower boundary of the convection zone is at point 173.